

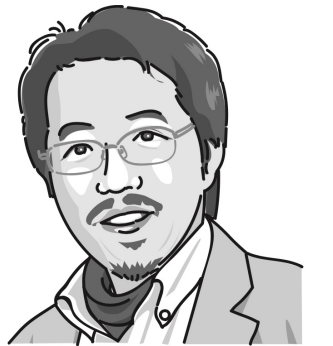
Gravitational wave and test of general relativity

Planned Contents

- ◆ GW projects: KAGRA
- ◆ LIGO-Virgo: GWTC-2 release & Test of GR
- ◆ Auto-Regressive method for data analysis

Hisaaki Shinkai (Osaka Inst. Tech.)

<http://www.oit.ac.jp/is/shinkai/>



HS, Kei-ichi Maeda, Andy Birkin, Nobuyuki Sakai

◀ In 1989, when Kei-ichi Maeda started a group at Waseda.

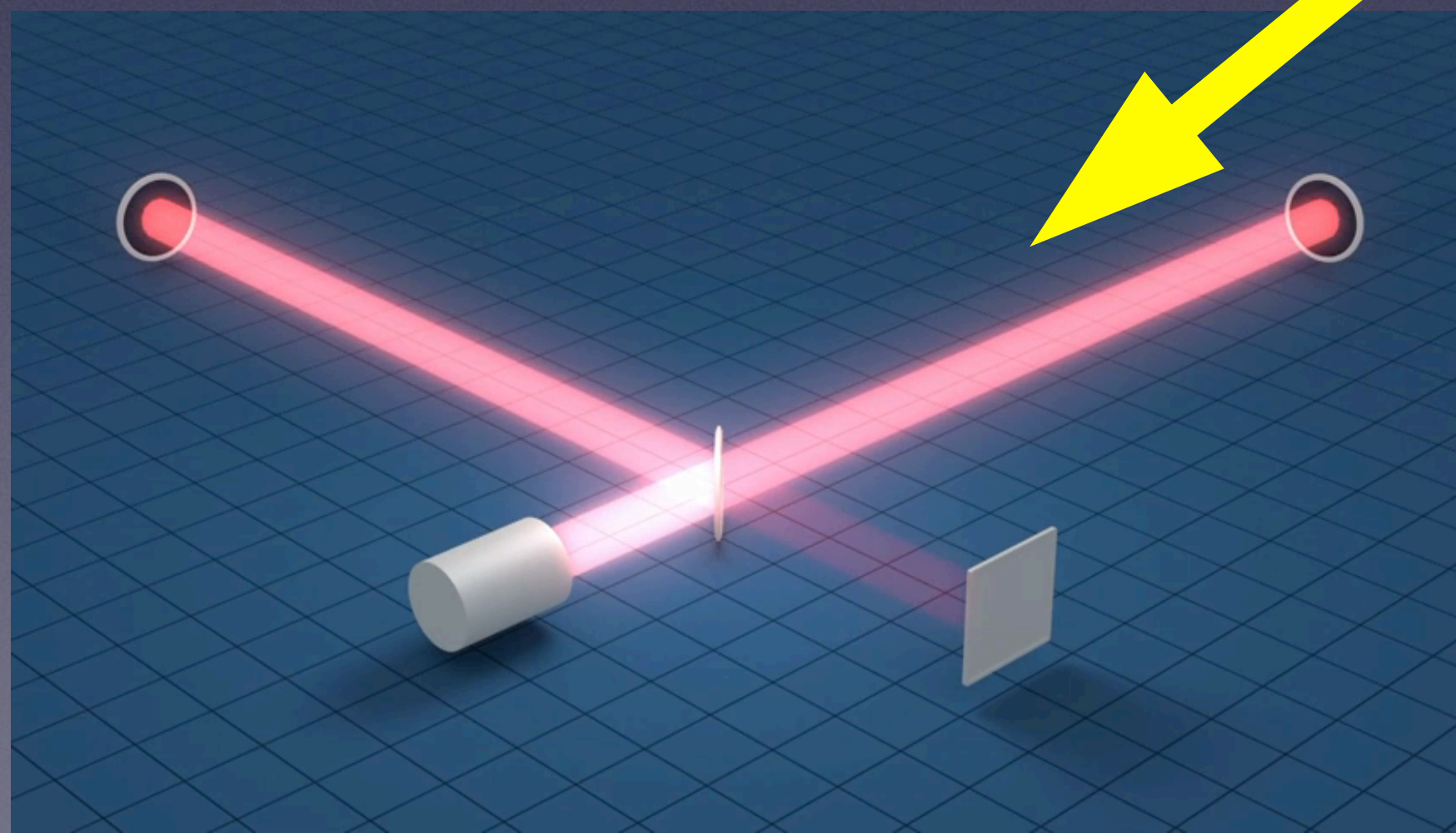
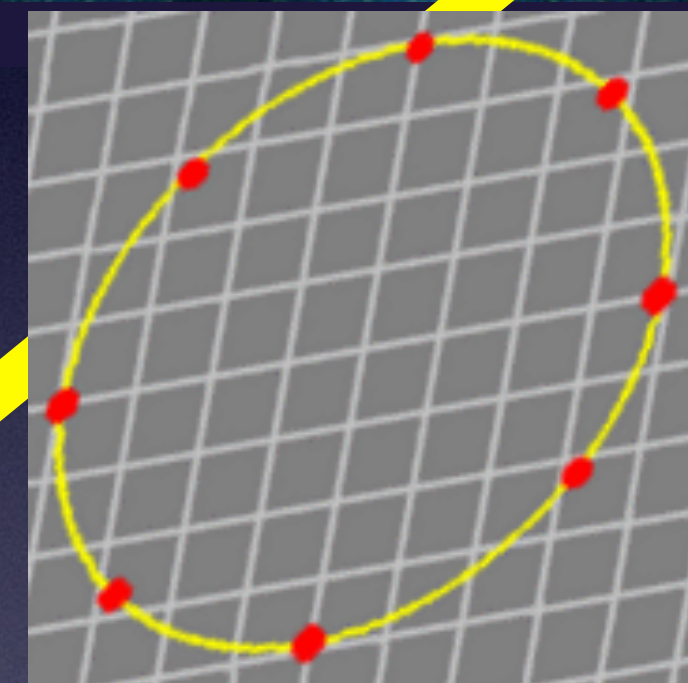
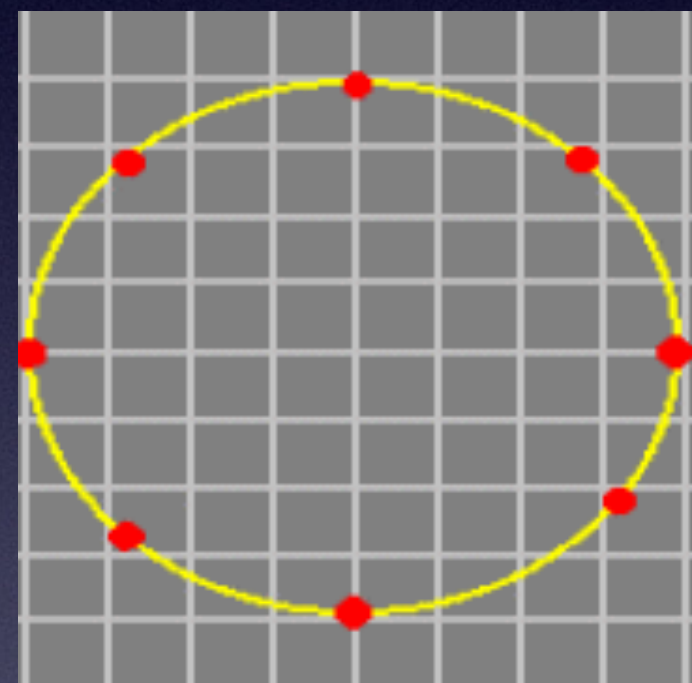
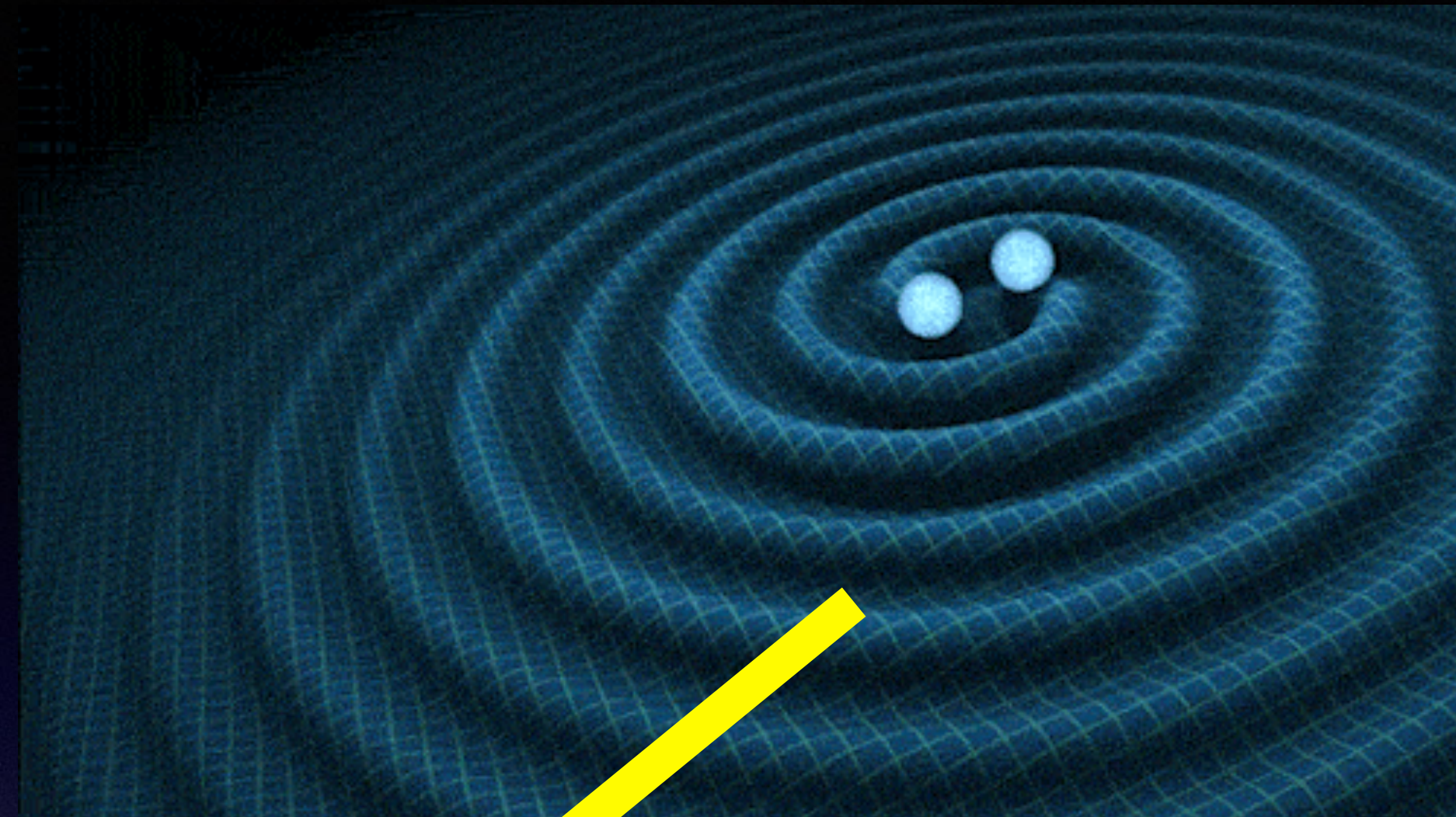
Kei-ichi suggested me to work in numerical relativity.

My thesis was on numerical analysis on the generality of inflationary cosmology.

I mainly worked formulation problem in NR, simulations in modified gravity theories, ... and now in GW data analysis.

Gravitational Wave

from binary BH-BH, NS-NS, BH-NS



GW International Network

4 km



4 km



600 m



3 km



3 km

KAGRA

◆ Underground and Cryogenic interferometric 3 km gravitational-wave detector at Kamioka, Japan



112 groups, 14 countries/regions
410+ active members

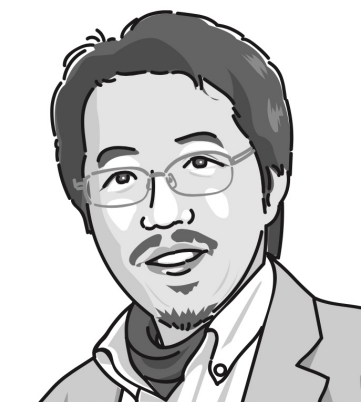
<http://gwwiki.icrr.u-tokyo.ac.jp/JGWwiki/KAGRA>



Takaaki Kajita (PI)

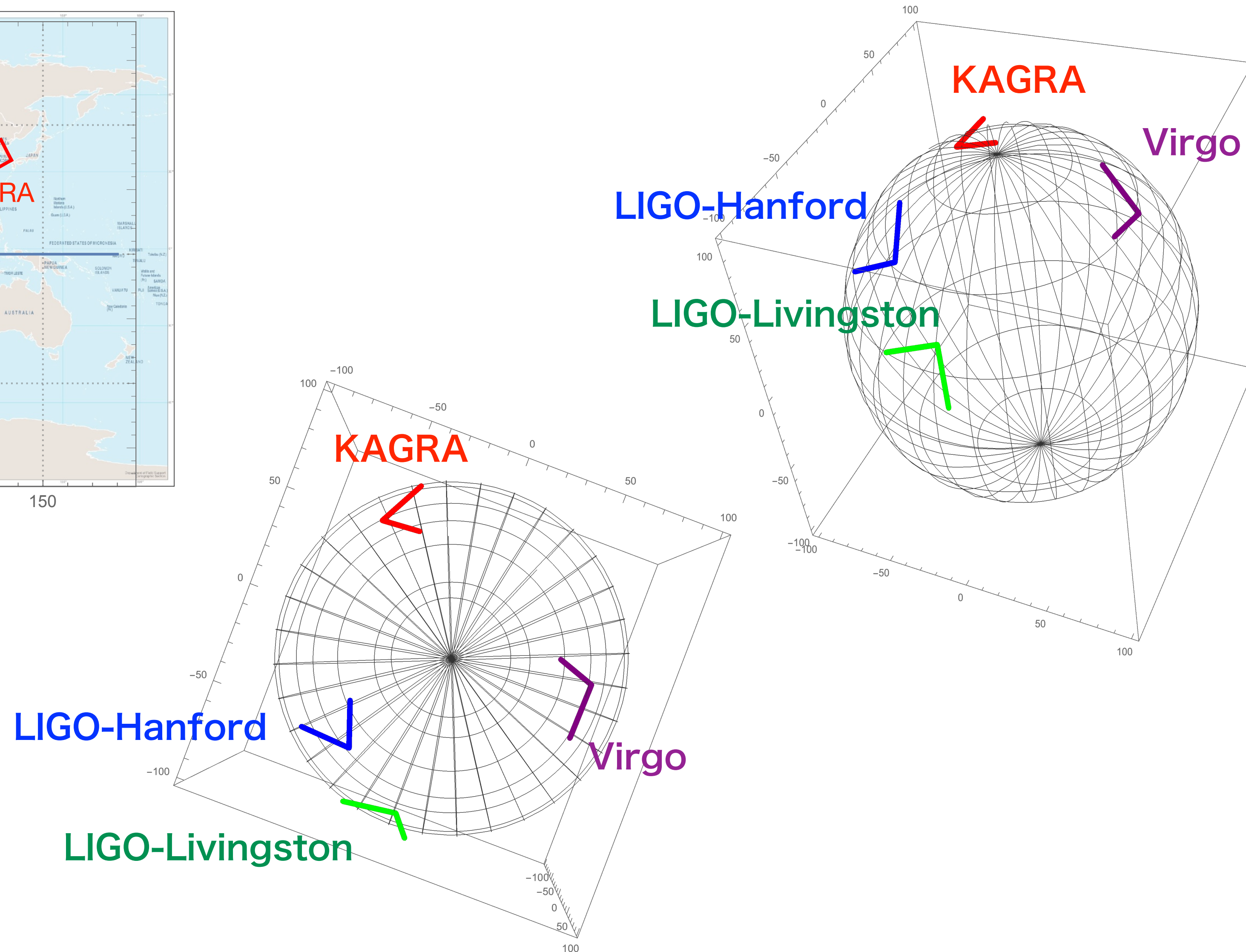
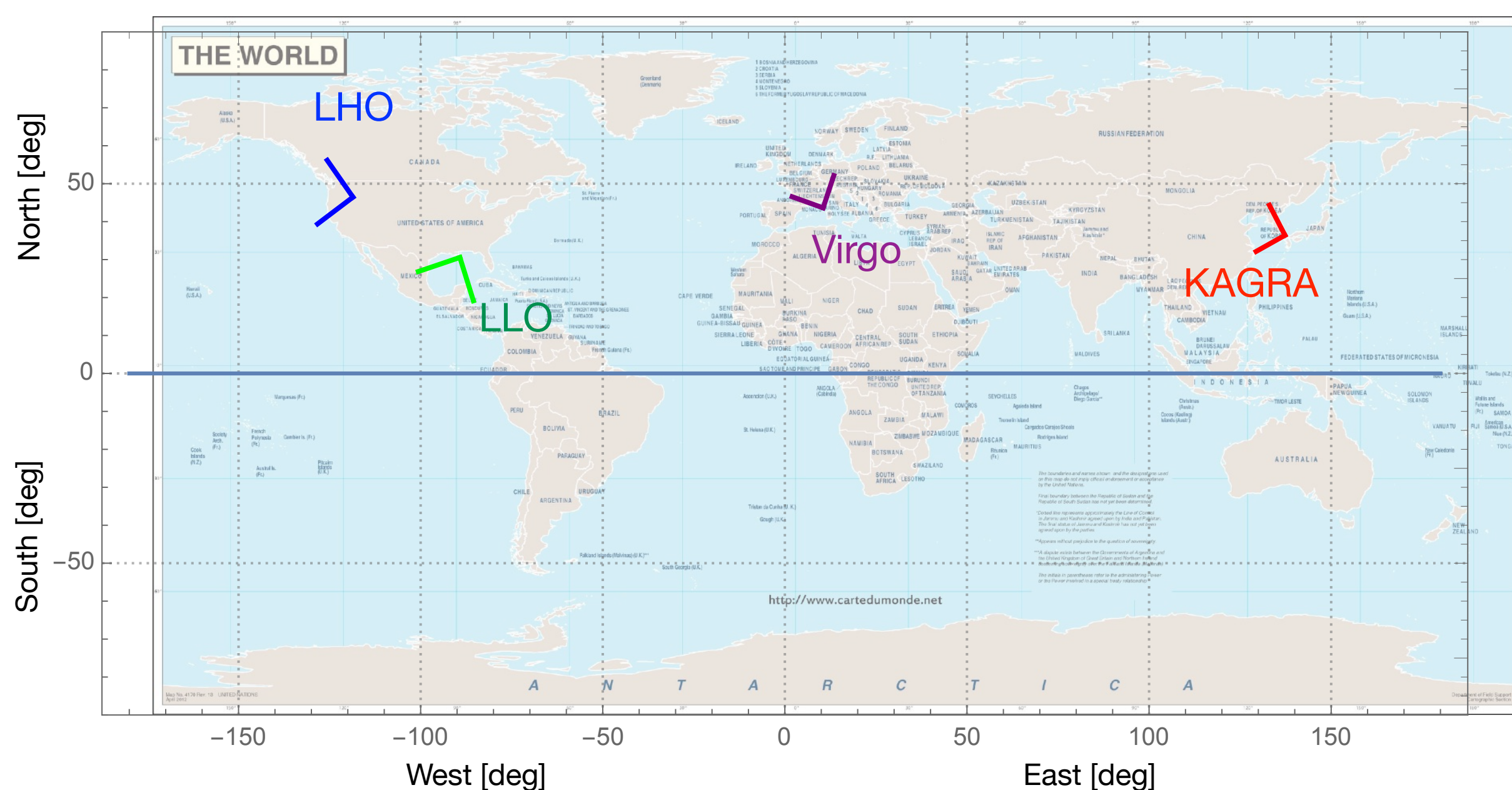


Masatake Ohashi (vice PI)



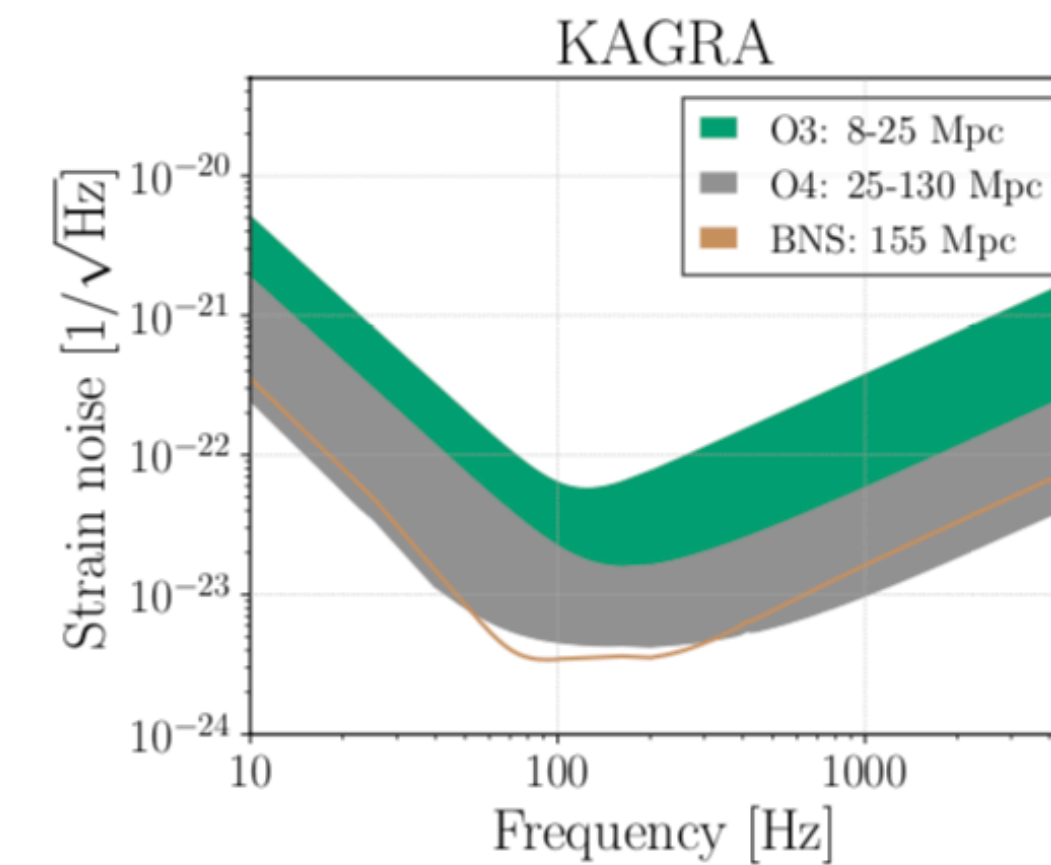
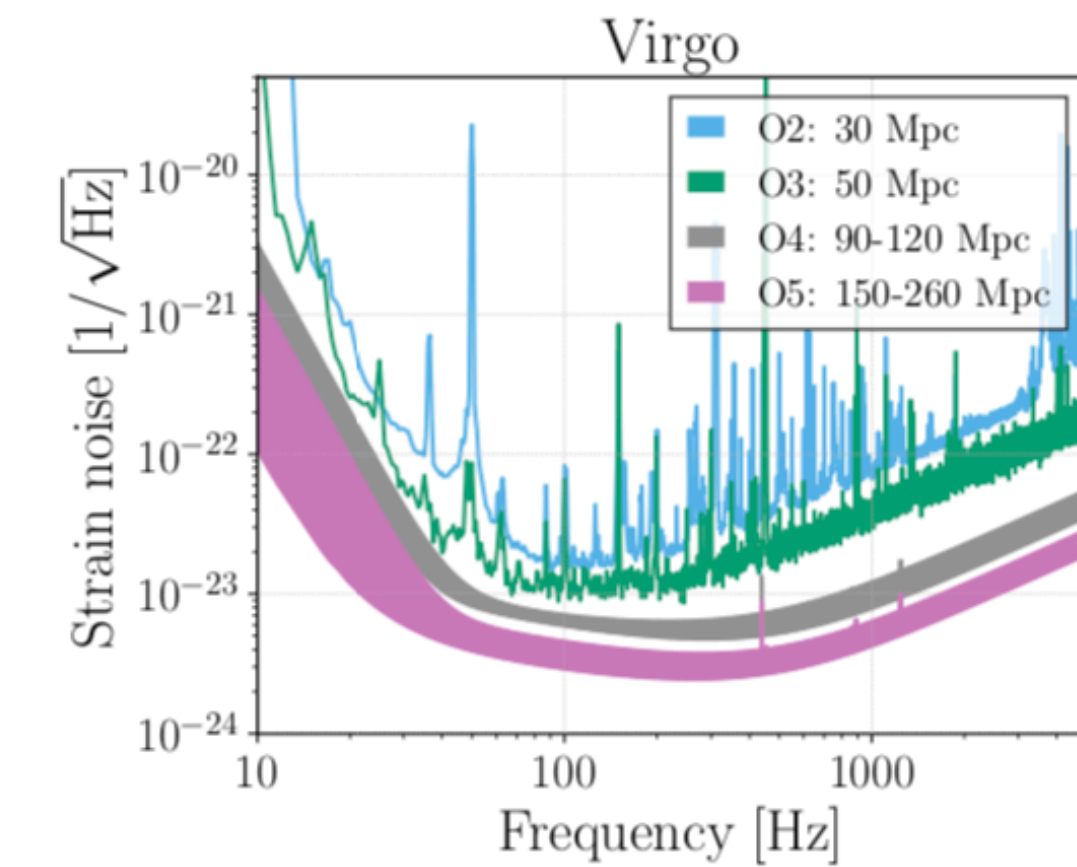
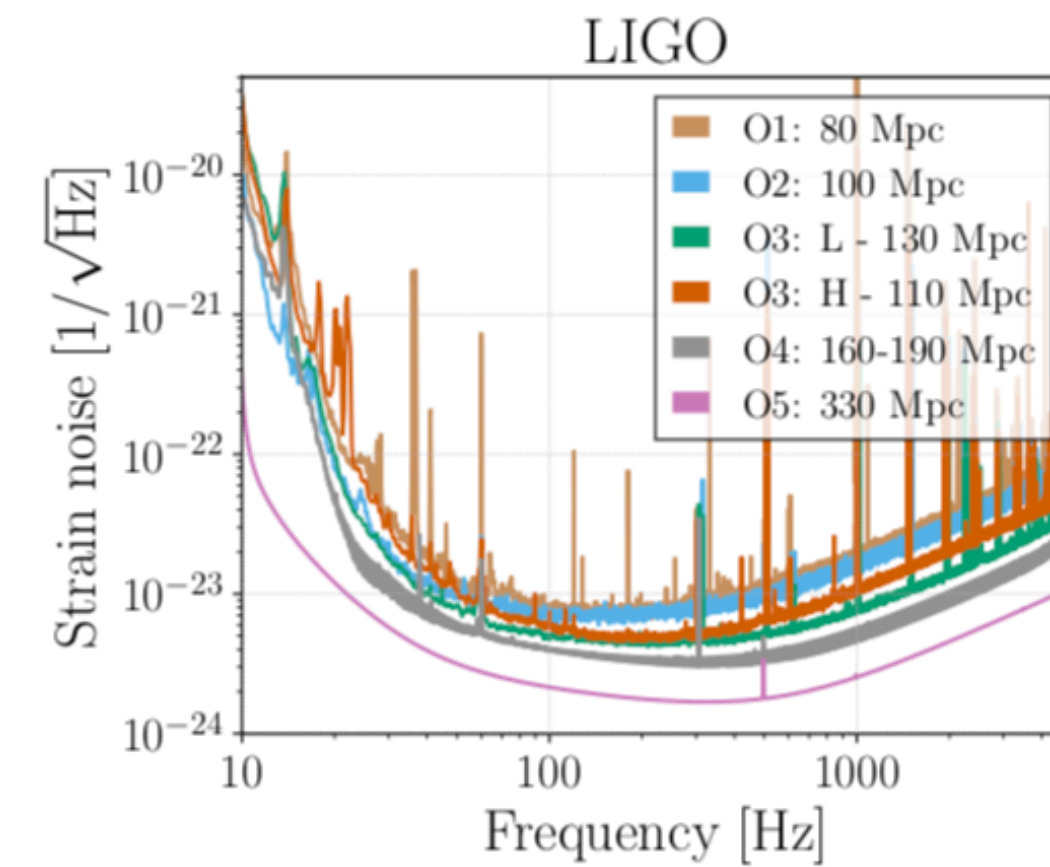
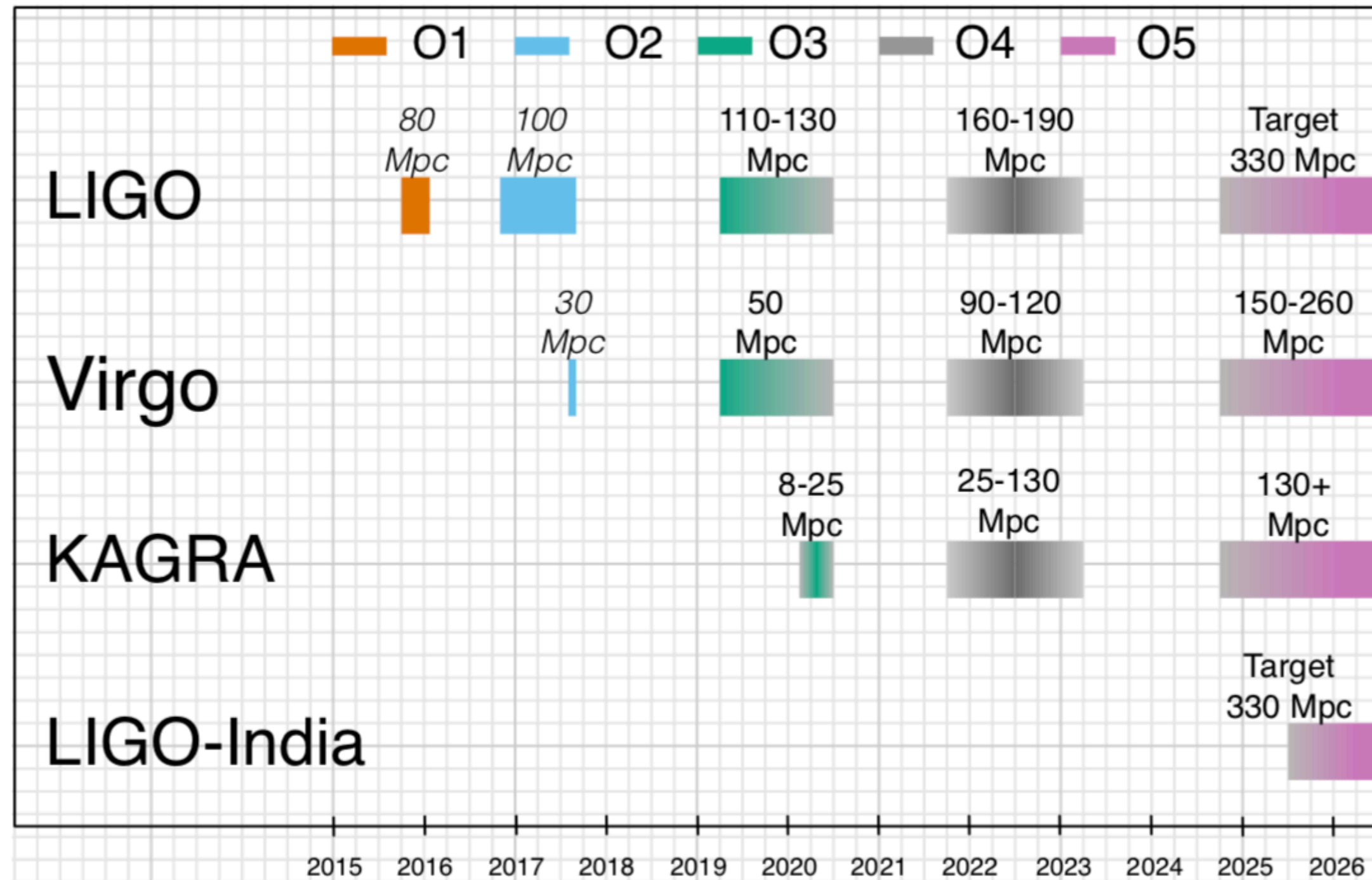
HS
board chair of KAGRA Scientific Congress
(2017-2021)

Fourth 2nd generation detector on the Earth



- more precise GW source localization
- more certain GW source parameters
- more chances to hunt GW events
- more ideas for GW researches
- more man power

Target Sensitivity & Schedule



“Scenario Paper” [1304.0670ver2020Jan]

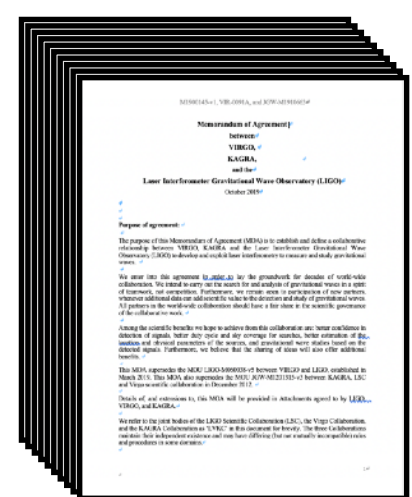
LVK collaboration, Living Rev Relativ (2020) 23:3

<https://link.springer.com/article/10.1007/s41114-020-00026-9>

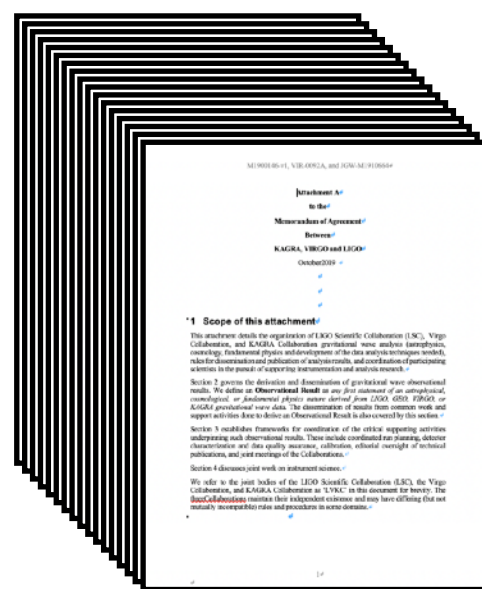
Joint Research MoA signed LIGO-Virgo-KAGRA



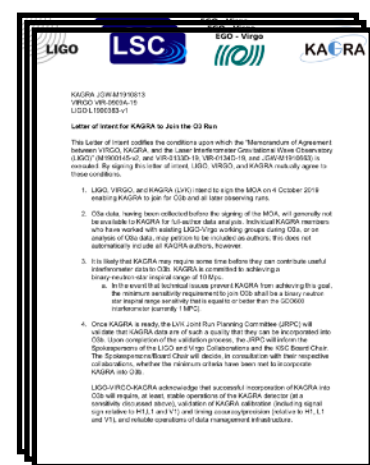
October 4, 2019 @ Ceremony of MoA signing



main part (10 pages)
Concept, Definitions,
Purposes

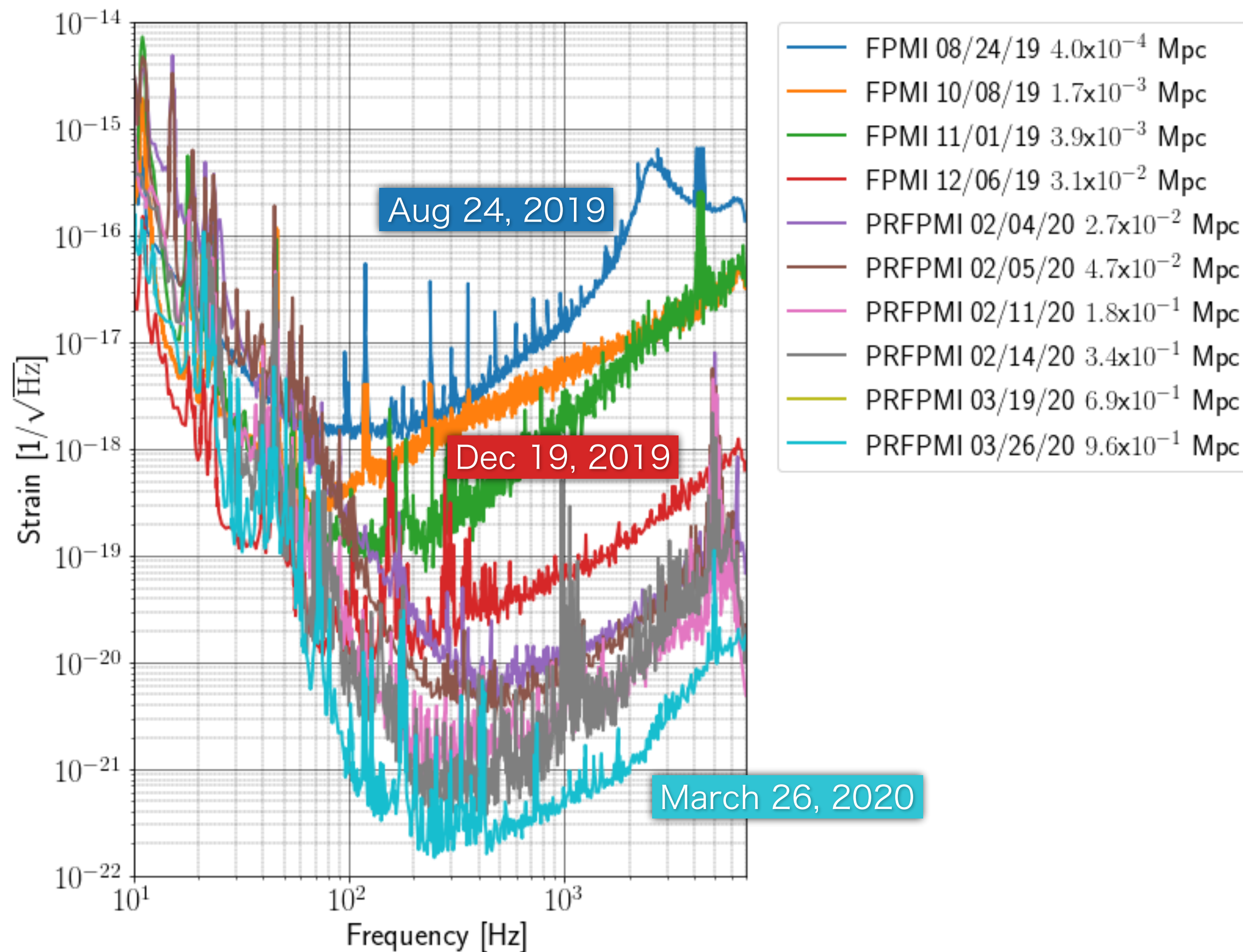


Appendix A (17 pages)
Organizations, Procedures



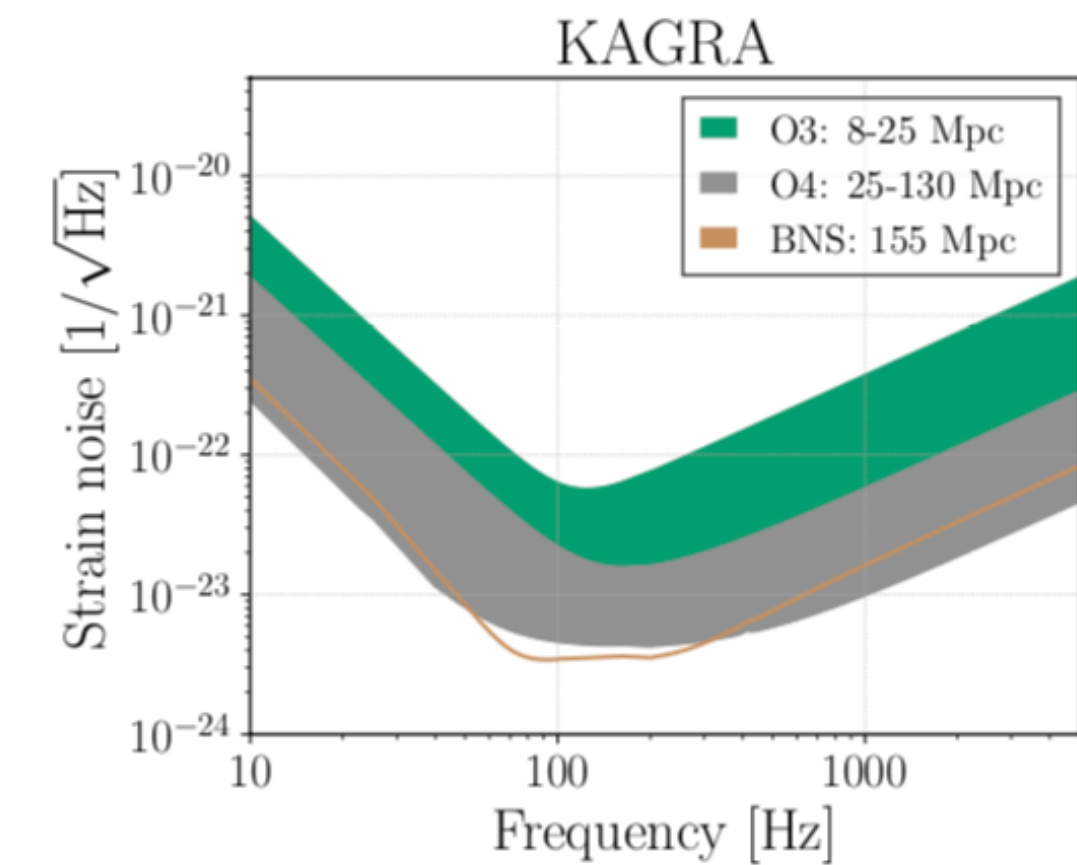
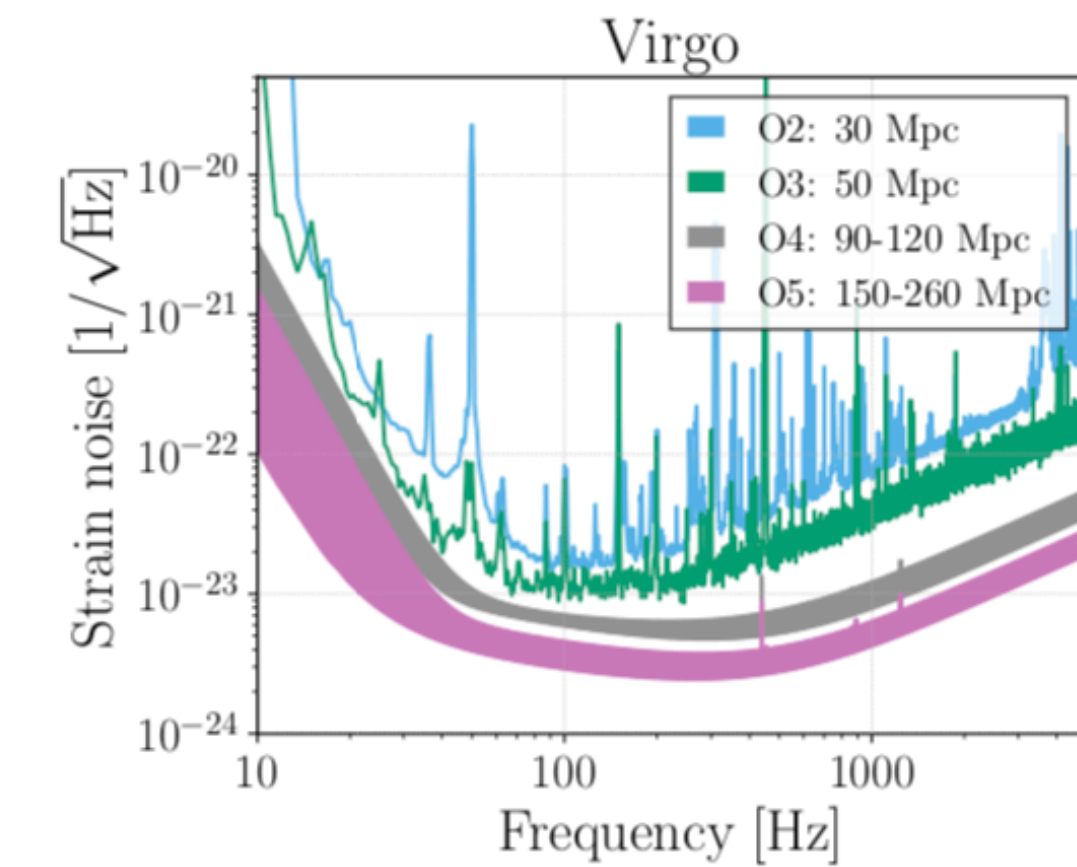
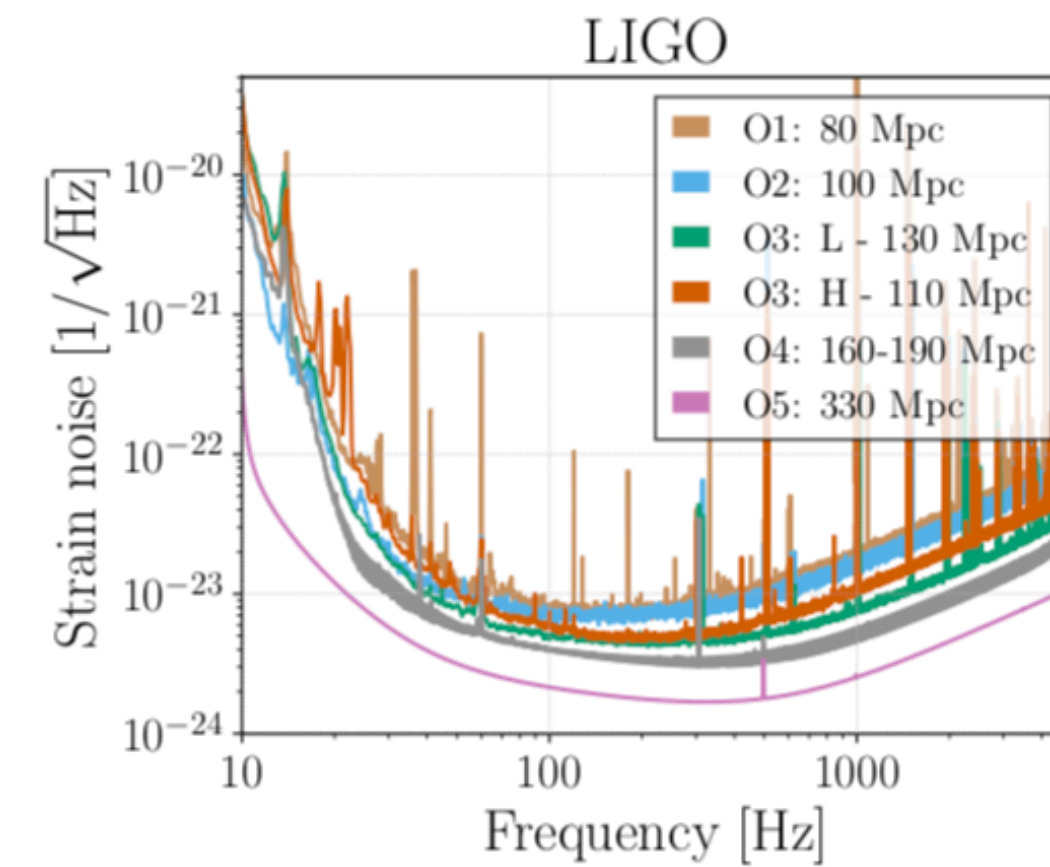
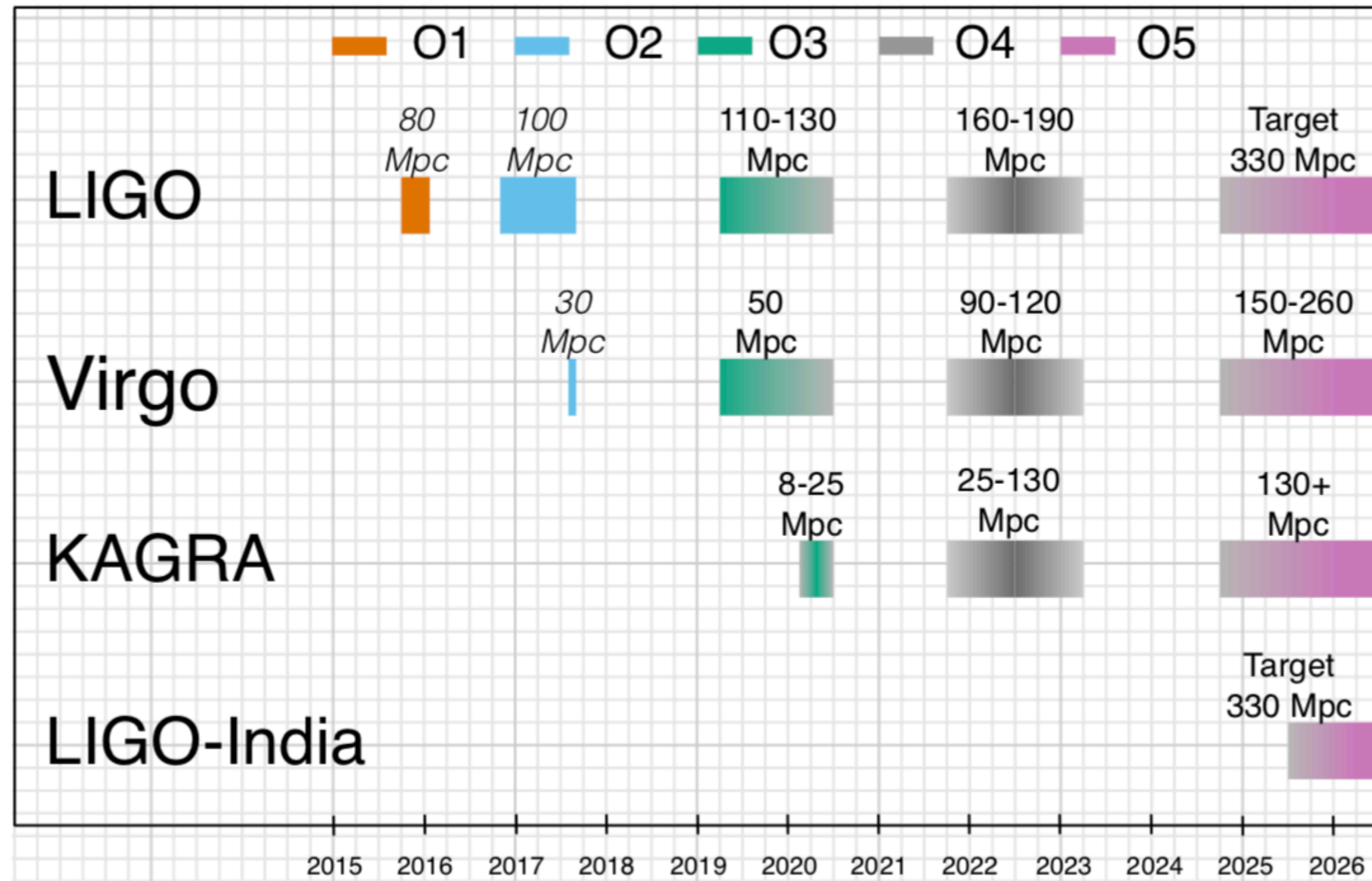
Letter of Intent (3 pages)
KAGRA's Join to O3

* 1 Mpc (BNS) is required to join the observation.



* Finally, over 1 Mpc in the end of March 26, 2020.

Target Sensitivity & Schedule

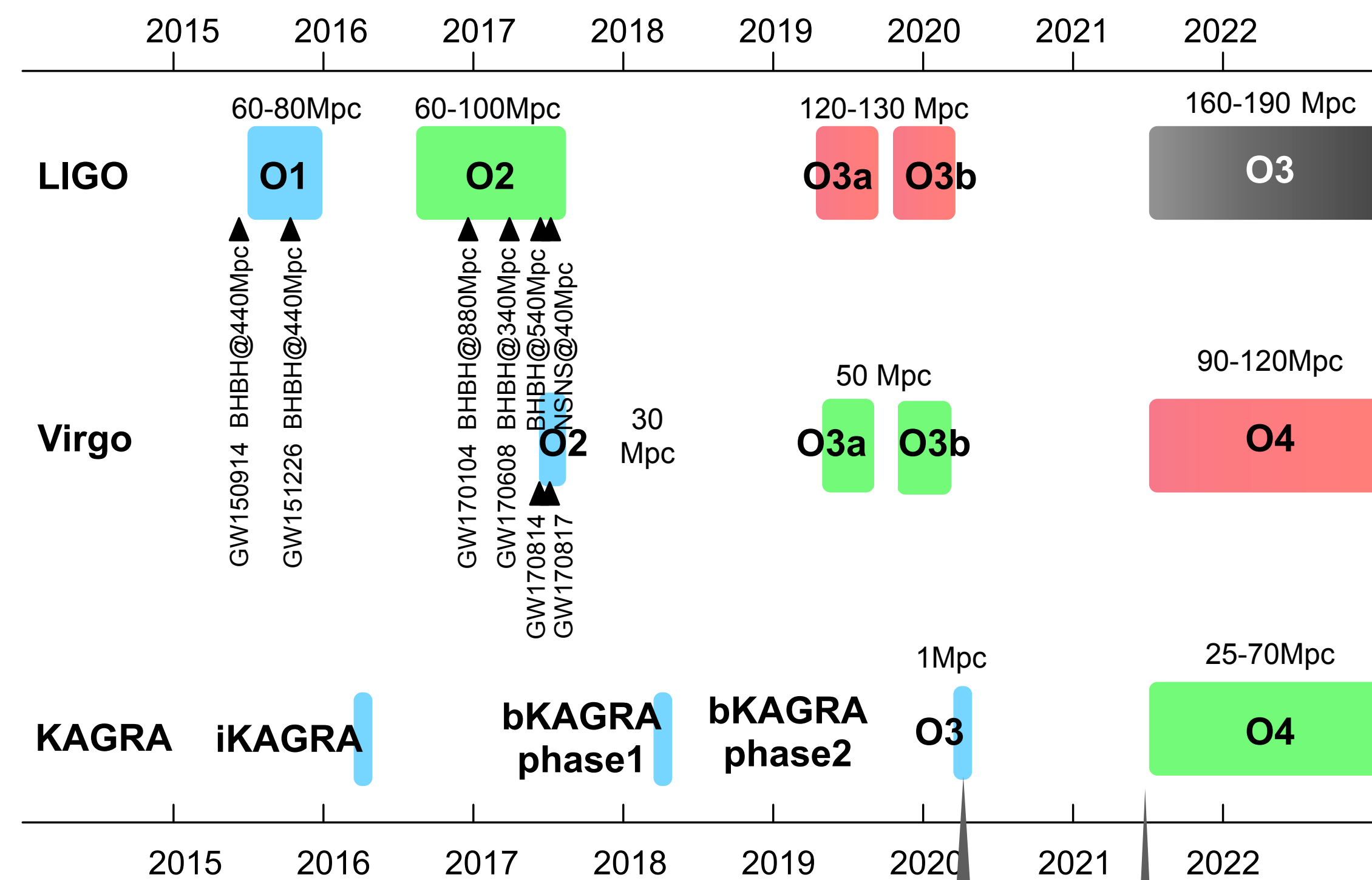
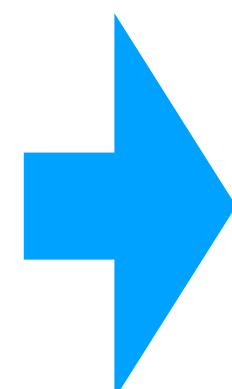
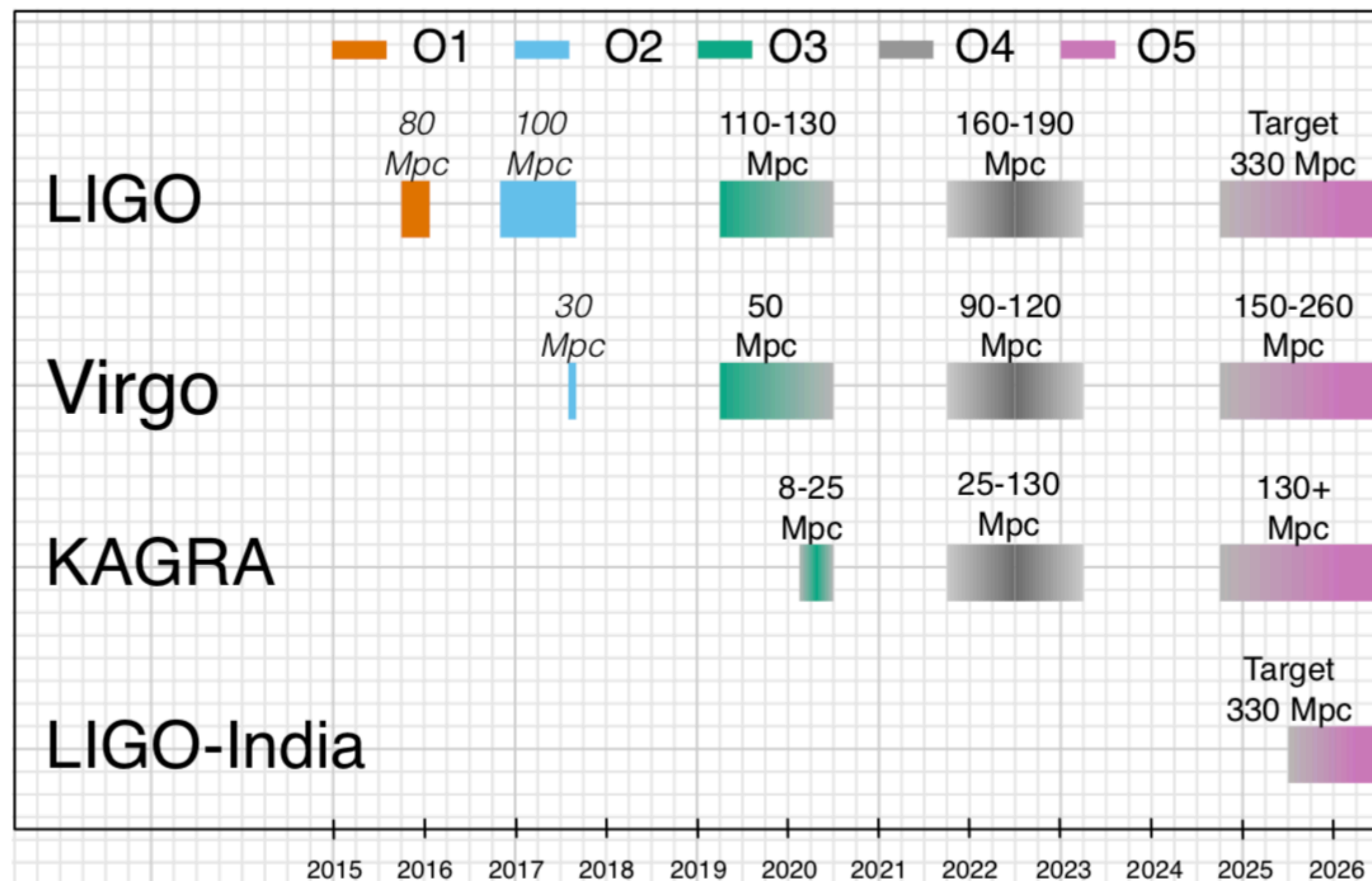


“Scenario Paper” [1304.0670ver2020Jan]

LVK collaboration, Living Rev Relativ (2020) 23:3

<https://link.springer.com/article/10.1007/s41114-020-00026-9>

Target Sensitivity & Schedule



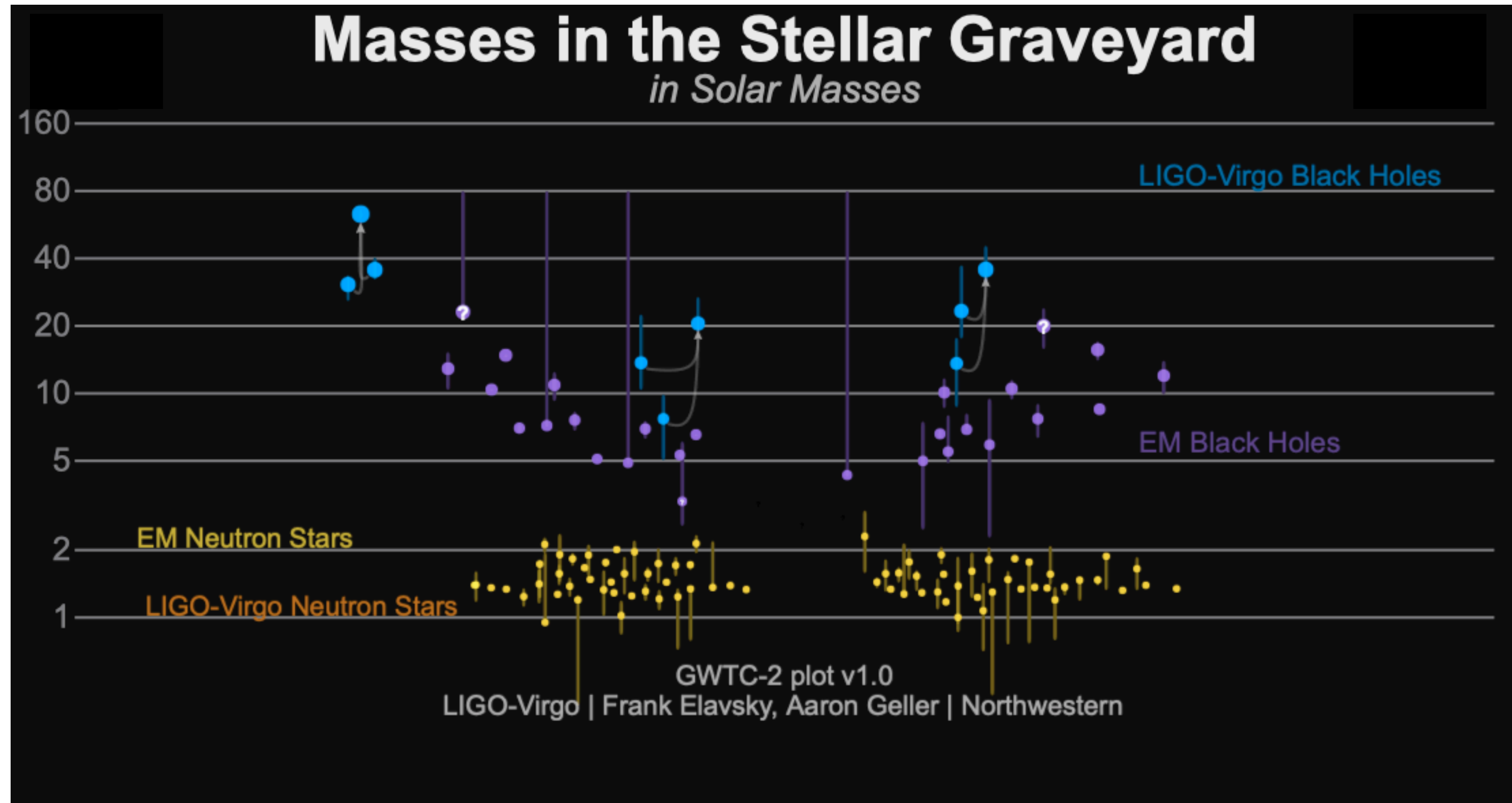
COVID-19 terminated O3b

O4 will likely start no earlier than June 2022

“Scenario Paper” [1304.0670ver2020Jan]

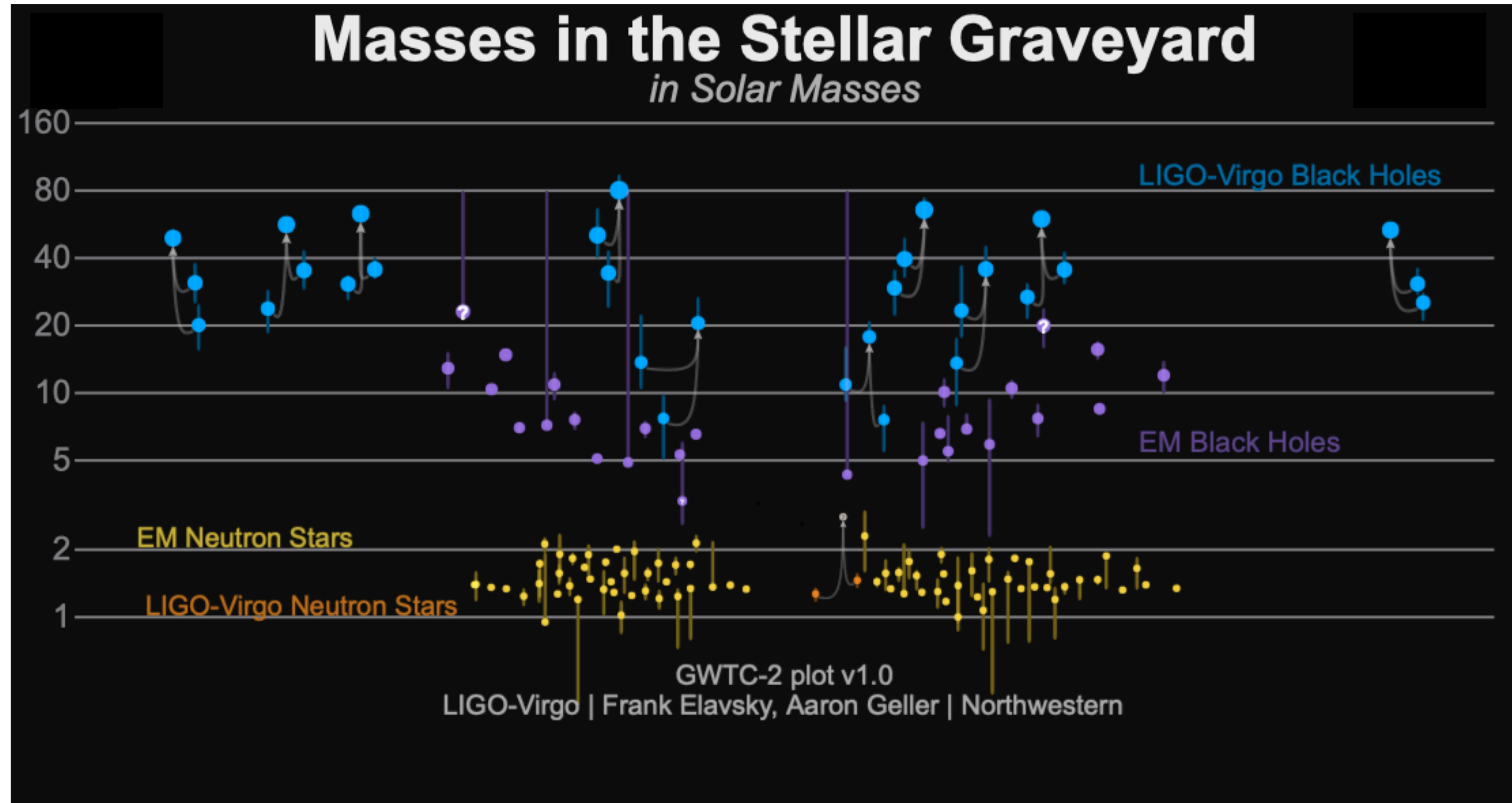
LVK collaboration, Living Rev Relativ (2020) 23:3
<https://link.springer.com/article/10.1007/s41114-020-00026-9>

O1 (2015/9/12 - 2016/1/19)

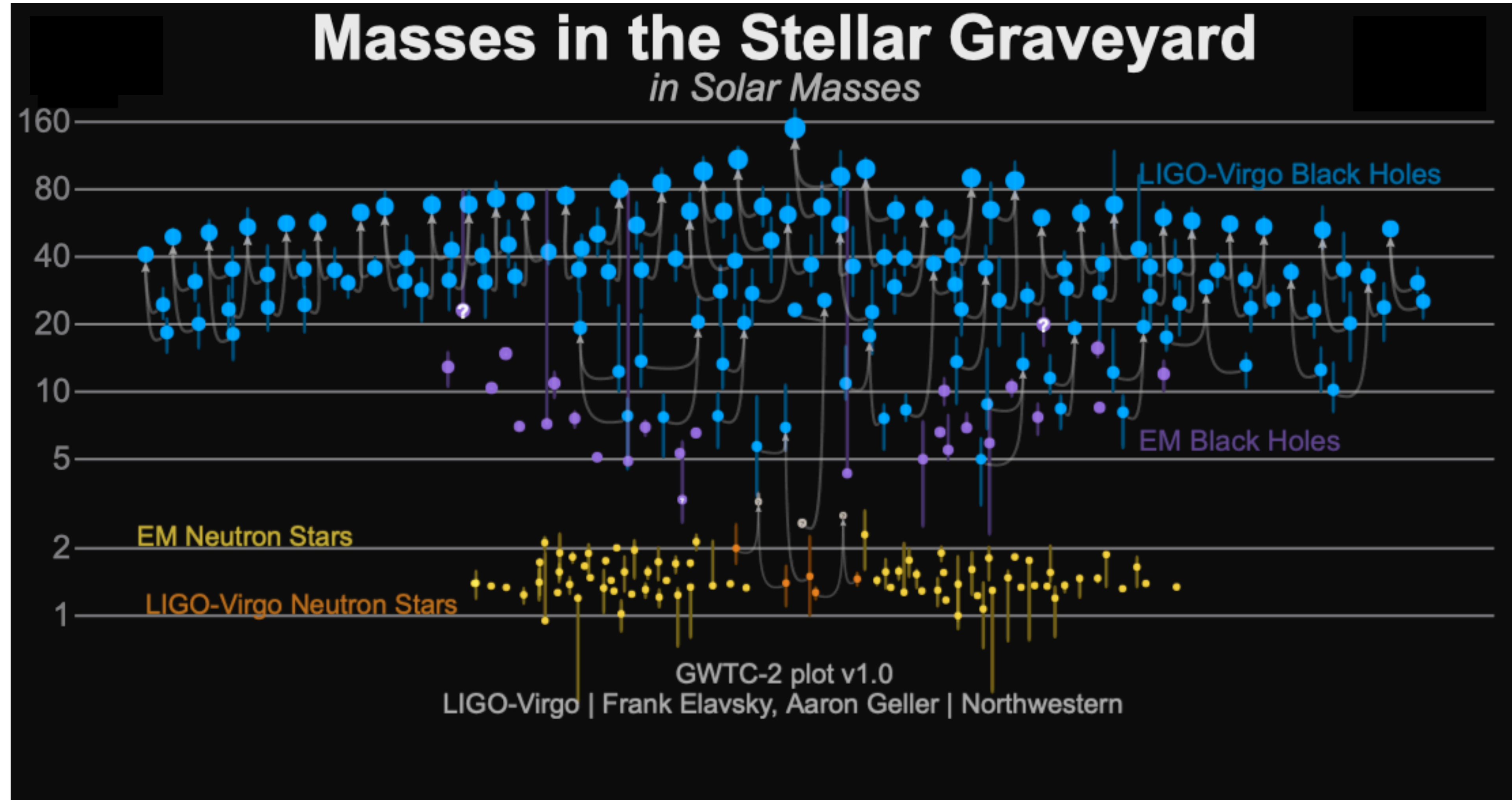


3 BHBH

GW150914: the first ever detection of gravitational waves from the merger of two black holes more than a billion light years away



- **GW170814**: the first GW signal measured by the three-detector network, also from a binary black hole (BBH) merger;
- **GW170817**: the first GW signal measured from a binary neutron star (BNS) merger — and also the first event observed in light, by dozens of telescopes across the entire electromagnetic spectrum.



46 BHBH
2 NSNS
2 BH+?

- [GW190412](#): the first BBH with definitively asymmetric component masses, which also shows evidence for [higher harmonics](#)
- [GW190425](#): the second gravitational-wave event consistent with a BNS, following [GW170817](#)
- [GW190426_152155](#): a low-mass event consistent with either an NSBH or BBH
- [GW190514_065416](#): a BBH with the smallest effective aligned spin of all O3a events
- [GW190517_055101](#): a BBH with the largest effective aligned spin of all O3a events
- [GW190521](#): a BBH with total mass over 150 times the mass of the Sun
- [GW190814](#): a highly asymmetric system of ambiguous nature, corresponding to the merger of a 23 solar mass black hole with a 2.6 solar mass compact object, making the latter either the lightest black hole or heaviest neutron star observed in a compact binary
- [GW190924_021846](#): likely the lowest-mass BBH, with both black holes exceeding 3 solar masses

GWTC-2

Gravitational Wave Transient Catalog 2

[arXiv:2010.14527](https://arxiv.org/abs/2010.14527)<https://dcc.ligo.org/LIGO-P2000223/public>

39 events in O3a

36BHBH, 1 NSNS, 2 BH+unknown

GWyymmdd_hhmmss for new events

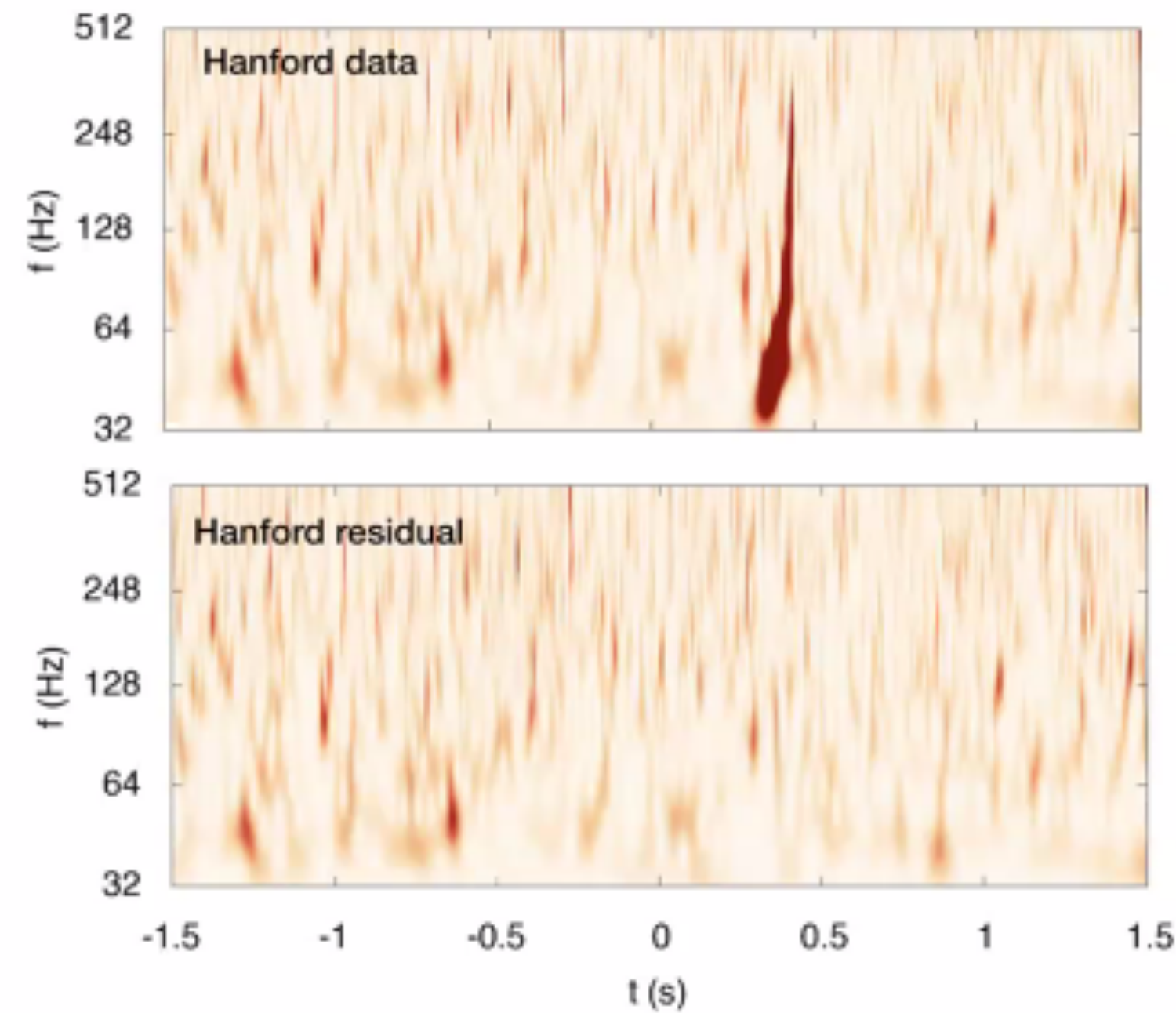
- [GW190412](#): the first BBH with definitively asymmetric component masses, which also shows evidence for [higher harmonics](#)
- [GW190425](#): the second gravitational-wave event consistent with a BNS, following [GW170817](#)
- [GW190426_152155](#): a low-mass event consistent with either an NSBH or BBH
- [GW190514_065416](#): a BBH with the smallest effective aligned spin of all O3a events
- [GW190517_055101](#): a BBH with the largest effective aligned spin of all O3a events
- [GW190521](#): a BBH with total mass over 150 times the mass of the Sun
- [GW190814](#): a highly asymmetric system of ambiguous nature, corresponding to the merger of a 23 solar mass black hole with a 2.6 solar mass compact object, making the latter either the lightest black hole or heaviest neutron star observed in a compact binary
- [GW190924_021846](#): likely the lowest-mass BBH, with both black holes exceeding 3 solar masses

[arXiv:2010.14529](https://arxiv.org/abs/2010.14529) Test of GR[arXiv:2010.14533](https://arxiv.org/abs/2010.14533) Population properties

Event	M (M_{\odot})	M (M_{\odot})	m_1 (M_{\odot})	m_2 (M_{\odot})	χ_{eff}	D_L (Gpc)	z	M_f (M_{\odot})	χ_f	$\Delta\Omega$ (deg 2)	SNR
GW190408_181802	42.9 $^{+4.1}_{-2.9}$	18.3 $^{+1.8}_{-1.2}$	24.5 $^{+5.1}_{-3.4}$	18.3 $^{+3.2}_{-3.5}$	-0.03 $^{+0.13}_{-0.19}$	1.58 $^{+0.40}_{-0.59}$	0.30 $^{+0.06}_{-0.10}$	41.0 $^{+3.8}_{-2.7}$	0.67 $^{+0.06}_{-0.07}$	140	15.3 $^{+0.2}_{-0.3}$
GW190412	38.4 $^{+3.8}_{-3.7}$	13.3 $^{+0.4}_{-0.3}$	30.0 $^{+4.7}_{-5.1}$	8.3 $^{+1.6}_{-0.9}$	0.25 $^{+0.08}_{-0.11}$	0.74 $^{+0.14}_{-0.17}$	0.15 $^{+0.03}_{-0.03}$	37.3 $^{+3.9}_{-3.9}$	0.67 $^{+0.05}_{-0.06}$	21	18.9 $^{+0.2}_{-0.3}$
GW190413_052954	56.9 $^{+13.1}_{-8.9}$	24.0 $^{+5.4}_{-3.7}$	33.4 $^{+12.4}_{-7.4}$	23.4 $^{+6.7}_{-6.3}$	0.01 $^{+0.29}_{-0.33}$	4.10 $^{+2.41}_{-1.89}$	0.66 $^{+0.30}_{-0.27}$	54.3 $^{+12.4}_{-8.4}$	0.69 $^{+0.12}_{-0.13}$	1400	8.9 $^{+0.4}_{-0.8}$
GW190413_134308	76.1 $^{+15.9}_{-10.6}$	31.9 $^{+7.3}_{-4.6}$	45.4 $^{+13.6}_{-9.6}$	30.9 $^{+10.2}_{-9.6}$	-0.01 $^{+0.24}_{-0.28}$	5.15 $^{+2.44}_{-2.34}$	0.80 $^{+0.30}_{-0.31}$	72.8 $^{+15.2}_{-10.3}$	0.69 $^{+0.10}_{-0.12}$	520	10.0 $^{+0.4}_{-0.5}$
GW190421_213856	71.8 $^{+12.5}_{-8.6}$	30.7 $^{+5.5}_{-3.9}$	40.6 $^{+10.4}_{-6.6}$	31.4 $^{+7.5}_{-8.2}$	-0.05 $^{+0.23}_{-0.26}$	3.15 $^{+1.37}_{-1.42}$	0.53 $^{+0.18}_{-0.21}$	68.6 $^{+11.7}_{-8.1}$	0.68 $^{+0.10}_{-0.11}$	1000	10.7 $^{+0.2}_{-0.4}$
GW190424_180648	70.7 $^{+13.4}_{-9.8}$	30.3 $^{+5.7}_{-4.2}$	39.5 $^{+10.9}_{-6.9}$	31.0 $^{+7.4}_{-7.3}$	0.15 $^{+0.22}_{-0.22}$	2.55 $^{+1.56}_{-1.33}$	0.45 $^{+0.22}_{-0.21}$	67.1 $^{+12.5}_{-9.2}$	0.75 $^{+0.08}_{-0.09}$	26000	10.4 $^{+0.2}_{-0.4}$
GW190425	3.4 $^{+0.3}_{-0.1}$	1.44 $^{+0.02}_{-0.02}$	2.0 $^{+0.6}_{-0.3}$	1.4 $^{+0.3}_{-0.3}$	0.06 $^{+0.11}_{-0.05}$	0.16 $^{+0.07}_{-0.07}$	0.03 $^{+0.01}_{-0.02}$	-	-	9900	12.4 $^{+0.3}_{-0.4}$
GW190426_152155	7.2 $^{+3.5}_{-1.5}$	2.41 $^{+0.08}_{-0.08}$	5.7 $^{+4.0}_{-2.3}$	1.5 $^{+0.8}_{-0.5}$	-0.03 $^{+0.33}_{-0.30}$	0.38 $^{+0.19}_{-0.16}$	0.08 $^{+0.04}_{-0.03}$	-	-	1400	8.7 $^{+0.5}_{-0.6}$
GW190503_185404	71.3 $^{+9.3}_{-8.0}$	30.1 $^{+4.2}_{-4.0}$	42.9 $^{+9.2}_{-7.8}$	28.5 $^{+7.5}_{-7.9}$	-0.02 $^{+0.20}_{-0.26}$	1.52 $^{+0.71}_{-0.66}$	0.29 $^{+0.11}_{-0.11}$	68.2 $^{+8.7}_{-7.5}$	0.67 $^{+0.09}_{-0.12}$	94	12.4 $^{+0.2}_{-0.3}$
GW190512_180714	35.6 $^{+3.9}_{-3.4}$	14.5 $^{+1.3}_{-1.0}$	23.0 $^{+5.4}_{-5.7}$	12.5 $^{+3.5}_{-2.5}$	0.03 $^{+0.13}_{-0.13}$	1.49 $^{+0.53}_{-0.59}$	0.28 $^{+0.09}_{-0.10}$	34.2 $^{+3.9}_{-3.4}$	0.65 $^{+0.07}_{-0.07}$	230	12.2 $^{+0.2}_{-0.4}$
GW190513_205428	53.6 $^{+8.6}_{-5.9}$	21.5 $^{+3.6}_{-1.9}$	35.3 $^{+9.6}_{-9.0}$	18.1 $^{+7.3}_{-4.2}$	0.12 $^{+0.29}_{-0.18}$	2.16 $^{+0.94}_{-0.80}$	0.39 $^{+0.14}_{-0.13}$	51.3 $^{+8.1}_{-5.8}$	0.69 $^{+0.14}_{-0.12}$	490	12.9 $^{+0.3}_{-0.4}$
GW190514_065416	64.2 $^{+16.6}_{-9.6}$	27.4 $^{+6.9}_{-4.3}$	36.9 $^{+13.4}_{-7.3}$	27.5 $^{+8.2}_{-7.7}$	-0.16 $^{+0.28}_{-0.32}$	4.93 $^{+2.76}_{-2.41}$	0.77 $^{+0.34}_{-0.33}$	61.6 $^{+16.0}_{-9.2}$	0.64 $^{+0.11}_{-0.14}$	2400	8.2 $^{+0.3}_{-0.6}$
GW190517_055101	61.9 $^{+10.0}_{-9.6}$	26.0 $^{+4.2}_{-4.0}$	36.4 $^{+11.8}_{-7.8}$	24.8 $^{+6.9}_{-7.1}$	0.53 $^{+0.20}_{-0.19}$	2.11 $^{+1.79}_{-1.00}$	0.38 $^{+0.26}_{-0.16}$	57.8 $^{+9.4}_{-9.1}$	0.87 $^{+0.05}_{-0.07}$	460	10.7 $^{+0.4}_{-0.6}$
GW190519_153544	104.2 $^{+14.5}_{-14.9}$	43.5 $^{+6.8}_{-6.8}$	64.5 $^{+11.3}_{-13.2}$	39.9 $^{+11.0}_{-10.6}$	0.33 $^{+0.19}_{-0.22}$	2.85 $^{+2.02}_{-1.14}$	0.49 $^{+0.27}_{-0.17}$	98.7 $^{+13.5}_{-14.2}$	0.80 $^{+0.07}_{-0.12}$	770	15.6 $^{+0.2}_{-0.3}$
GW190521	157.9 $^{+37.4}_{-20.9}$	66.9 $^{+15.5}_{-9.2}$	91.4 $^{+29.3}_{-17.5}$	66.8 $^{+20.7}_{-20.7}$	0.06 $^{+0.31}_{-0.37}$	4.53 $^{+2.30}_{-2.13}$	0.72 $^{+0.29}_{-0.29}$	150.3 $^{+35.8}_{-20.0}$	0.73 $^{+0.11}_{-0.14}$	940	14.2 $^{+0.3}_{-0.3}$
GW190521_074359	74.4 $^{+6.8}_{-4.6}$	31.9 $^{+3.1}_{-2.4}$	42.1 $^{+5.9}_{-4.9}$	32.7 $^{+5.4}_{-6.2}$	0.09 $^{+0.10}_{-0.13}$	1.28 $^{+0.38}_{-0.57}$	0.25 $^{+0.06}_{-0.10}$	70.7 $^{+6.4}_{-4.2}$	0.72 $^{+0.05}_{-0.07}$	500	25.8 $^{+0.1}_{-0.2}$
GW190527_092055	58.5 $^{+27.9}_{-10.6}$	24.2 $^{+11.9}_{-4.4}$	36.2 $^{+19.1}_{-9.5}$	22.8 $^{+12.7}_{-8.1}$	0.13 $^{+0.29}_{-0.28}$	3.10 $^{+4.85}_{-1.64}$	0.53 $^{+0.61}_{-0.25}$	55.9 $^{+26.4}_{-10.1}$	0.73 $^{+0.12}_{-0.16}$	3800	8.1 $^{+0.4}_{-1.0}$
GW190602_175927	114.1 $^{+18.5}_{-15.7}$	48.3 $^{+8.6}_{-8.0}$	67.2 $^{+16.0}_{-12.6}$	47.4 $^{+13.4}_{-16.6}$	0.10 $^{+0.25}_{-0.25}$	2.99 $^{+2.02}_{-1.26}$	0.51 $^{+0.27}_{-0.19}$	108.8 $^{+17.2}_{-14.8}$	0.71 $^{+0.10}_{-0.13}$	720	12.8 $^{+0.2}_{-0.3}$
GW190620_030421	90.1 $^{+17.3}_{-12.1}$	37.5 $^{+7.8}_{-5.7}$	55.4 $^{+15.8}_{-12.0}$	35.0 $^{+11.6}_{-11.4}$	0.34 $^{+0.21}_{-0.25}$	3.16 $^{+1.67}_{-1.43}$	0.54 $^{+0.22}_{-0.21}$	85.4 $^{+15.9}_{-11.4}$	0.80 $^{+0.08}_{-0.14}$	6700	12.1 $^{+0.3}_{-0.4}$
GW190630_185205	58.8 $^{+4.7}_{-4.8}$	24.8 $^{+2.1}_{-2.0}$	35.0 $^{+6.9}_{-5.7}$	23.6 $^{+5.2}_{-5.1}$	0.10 $^{+0.12}_{-0.13}$	0.93 $^{+0.56}_{-0.40}$	0.19 $^{+0.10}_{-0.07}$	56.1 $^{+4.5}_{-4.6}$	0.70 $^{+0.06}_{-0.07}$	1300	15.6 $^{+0.2}_{-0.3}$
GW190701_203306	94.1 $^{+11.6}_{-9.3}$	40.2 $^{+5.2}_{-4.7}$	53.6 $^{+11.7}_{-7.8}$	40.8 $^{+8.3}_{-11.5}$	-0.06 $^{+0.23}_{-0.28}$	2.14 $^{+0.79}_{-0.73}$	0.38 $^{+0.12}_{-0.12}$	90.0 $^{+10.8}_{-8.6}$	0.67 $^{+0.09}_{-0.12}$	45	11.3 $^{+0.2}_{-0.4}$
GW190706_222641	101.6 $^{+17.9}_{-13.5}$	42.0 $^{+8.4}_{-6.2}$	64.0 $^{+15.2}_{-15.2}$	38.5 $^{+12.5}_{-12.4}$	0.32 $^{+0.25}_{-0.30}$	5.07 $^{+2.57}_{-2.11}$	0.79 $^{+0.31}_{-0.28}$	96.3 $^{+16.7}_{-13.2}$	0.80 $^{+0.08}_{-0.17}$	610	12.6 $^{+0.2}_{-0.4}$
GW190707_093326	20.0 $^{+1.9}_{-1.3}$	8.5 $^{+0.6}_{-0.4}$	11.5 $^{+3.3}_{-1.7}$	8.4 $^{+1.4}_{-1.6}$	-0.05 $^{+0.10}_{-0.08}$	0.80 $^{+0.37}_{-0.38}$	0.16 $^{+0.07}_{-0.07}$	19.2 $^{+1.9}_{-1.3}$	0.66 $^{+0.03}_{-0.04}$	1300	13.3 $^{+0.2}_{-0.4}$
GW190708_232457	30.8 $^{+2.5}_{-1.8}$	13.1 $^{+0.9}_{-0.6}$	17.5 $^{+4.7}_{-2.3}$	13.1 $^{+2.0}_{-2.7}$	0.02 $^{+0.10}_{-0.08}$	0.90 $^{+0.33}_{-0.40}$	0.18 $^{+0.06}_{-0.07}$	29.4 $^{+2.5}_{-1.7}$	0.69 $^{+0.04}_{-0.04}$	14000	13.1 $^{+0.2}_{-0.3}$
GW190719_215514	55.8 $^{+16.3}_{-10.0}$	22.7 $^{+5.9}_{-3.7}$	35.2 $^{+16.9}_{-9.9}$	20.2 $^{+8.1}_{-6.5}$	0.35 $^{+0.28}_{-0.32}$	4.61 $^{+2.84}_{-2.17}$	0.73 $^{+0.35}_{-0.30}$	52.9 $^{+15.6}_{-9.5}$	0.80 $^{+0.10}_{-0.16}$	2300	8.3 $^{+0.3}_{-1.0}$
GW190720_000836	21.3 $^{+4.3}_{-2.3}$	8.9 $^{+0.5}_{-0.8}$	13.3 $^{+6.6}_{-3.0}$	7.8 $^{+2.2}_{-2.2}$	0.18 $^{+0.14}_{-0.12}$	0.81 $^{+0.71}_{-0.33}$	0.16 $^{+0.12}_{-0.06}$	20.3 $^{+4.5}_{-2.3}$	0.72 $^{+0.06}_{-0.05}$	510	11.0 $^{+0.3}_{-0.8}$
GW190727_060333	65.8 $^{+10.9}_{-7.4}$	28.1 $^{+4.9}_{-3.4}$	37.2 $^{+9.4}_{-5.9}$	28.8 $^{+6.6}_{-7.9}$	0.12 $^{+0.26}_{-0.25}$	3.60 $^{+1.56}_{-1.51}$	0.60 $^{+0.20}_{-0.22}$	62.6 $^{+10.2}_{-7.0}$	0.73 $^{+0.10}_{-0.10}$	860	11.9 $^{+0.3}_{-0.5}$
GW190728_064510	20.5 $^{+4.5}_{-1.3}$	8.6 $^{+0.5}_{-0.3}$	12.2 $^{+7.1}_{-2.2}$	8.1 $^{+1.7}_{-2.6}$	0.12 $^{+0.19}_{-0.07}$	0.89 $^{+0.25}_{-0.37}$	0.18 $^{+0.05}_{-0.07}$	19.5 $^{+4.6}_{-1.3}$	0.71 $^{+0.04}_{-0.04}$	410	13.0 $^{+0.2}_{-0.4}$
GW190731_140936	67.1 $^{+15.3}_{-10.2}$	28.4 $^{+6.8}_{-4.5}$	39.3 $^{+11.8}_{-8.2}$	28.0 $^{+8.9}_{-8.4}$	0.08 $^{+0.24}_{-0.24}$	3.97 $^{+2.56}_{-2.07}$	0.65 $^{+0.32}_{-0.30}$	63.9 $^{+14.4}_{-9.8}$	0.71 $^{+0.10}_{-0.12}$	3000	8.6 $^{+0.2}_{-0.5}$
GW190803_022701	62.7 $^{+11.8}_{-8.4}$	26.7 $^{+5.2}_{-3.8}$	36.1 $^{+10.2}_{-6.7}$	26.7 $^{+7.1}_{-7.6}$	-0.01 $^{+0.25}_{-0.26}$	3.69 $^{+2.04}_{-1.69}$	0.61 $^{+0.26}_{-0.24}$	59.9 $^{+11.2}_{-7.9}$	0.69 $^{+0.10}_{-0.11}$	1500	8.6 $^{+0.3}_{-0.5}$
GW190814	25.8 $^{+1.0}_{-0.9}$	6.09 $^{+0.06}_{-0.06}$	23.2 $^{+1.1}_{-1.0}$	2.59 $^{+0.08}_{-0.09}$	0.00 $^{+0.06}_{-0.06}$	0.24 $^{+0.04}_{-0.05}$	0.05 $^{+0.009}_{-0.010}$	25.6 $^{+1.0}_{-0.9}$	0.28 $^{+0.02}_{-0.02}$	19	24.9 $^{+0.1}_{-0.2}$
GW190828_063405	57.5 $^{+7.5}_{-4.4}$	24.8 $^{+3.3}_{-2.0}$	31.8 $^{+5.8}_{-3.9}$	25.9 $^{+4.4}_{-4.6}$	0.19 $^{+0.15}_{-0.16}$	2.22 $^{+0.63}_{-0.95}$	0.40 $^{+0.09}_{-0.15}$	54.5 $^{+6.9}_{-4.0}$	0.76 $^{+0.06}_{-0.07}$	520	16.2 $^{+0.2}_{-0.3}$
GW190828_065509	34.1 $^{+5.5}_{-4.5}$	13.3 $^{+1.2}_{-0.9}$	23.8 $^{+7.2}_{-7.0}$	10.2 $^{+3.5}_{-2.1}$	0.08 $^{+0.16}_{-0.16}$	1.66 $^{+0.63}_{-0.61}$	0.31 $^{+0.10}_{-0.10}$	32.9 $^{+5.7}_{-4.5}$	0.65 $^{+0.09}_{-0.08}$	640	10.0 $^{+0.3}_{-0.5}$
GW190909_114149	71.2 $^{+54.3}_{-15.0}$	29.5 $^{+17.5}_{-12.2}$	43.2 $^{+50.7}_{-10.9}$	27.6 $^{+13.0}_{-10.9}$	-0.03 $^{+0.44}_{-0.36}$	4.77 $^{+3.70}_{-2.66}$	0.75 $^{+0.45}_{-0.37}$	68.3 $^{+52.5}_{-14.5}$	0.68 $^{+0.16}_{-0.18}$	4200	8.1 $^{+0.4}_{-0.7}$
GW190910_112807	78.7 $^{+9.5}_{-9.0}$	33.9 $^{+4.3}_{-3.9}$	43.5 $^{+7.6}_{-6.2}$	35.1 $^{+6.3}_{-7.0}$	0.02 $^{+0.19}_{-0.18}$	1.57 $^{+1.07}_{-0.64}$	0.29 $^{+0.17}_{-0.11}$	75.0 $^{+8.7}_{-8.5}$	0.70 $^{+0.08}_{-0.07}$	10000	14.1 $^{+0.2}_{-0.3}$
GW190915_235702	59.5 $^{+7.5}_{-6.2}$	25.1 $^{+3.1}_{-2.6}$	34.9 $^{+9.5}_{-6.2}$	24.4 $^{+5.5}_{-6.0}$	0.03 $^{+0.19}_{-0.24}$	1.70 $^{+0.71}_{-0.64}$	0.32 $^{+0.11}_{-0.11}$	56.8 $^{+7.1}_{-5.8}$	0.71 $^{+0.09}_{-0.11}$	380	13.6 $^{+0.2}_{-0.3}$
GW190924_021846	13.9 $^{+5.1}_{-0.9}$	5.8 $^{+0.2}_{-0.2}$	8.8 $^{+7.0}_{-2.0}$	5.0 $^{+1.3}_{-1.9}$	0.03 $^{+0.30}_{-0.09}$	0.57 $^{+0.22}_{-0.22}$	0.12 $^{+0.04}_{-0.04}$	13.3 $^{+5.2}_{-1.0}$	0.67 $^{+0.05}_{-0.05}$	380	11.5 $^{+0.3}_{-0.4}$
GW190929_012149	90.6 $^{+21.2}_{-14.1}$	34.3 $^{+8.6}_{-6.5}$	64.7 $^{+22.4}_{-18.9}$	25.7 $^{+14.4}_{-9.7}$	0.03 $^{+0.27}_{-0.27}$	3.68 $^{+2.98}_{-1.68}$	0.61 $^{+0.38}_{-0.24}$	87.5 $^{+20.7}_{-14.1}$	0.64 $^{+0.17}_{-0.23}$	1800	9.8 $^{+0.8}_{-0.6}$
GW190930_133541	20.3 $^{+9.0}_{-1.5}$	8.5 $^{+0.5}_{-0.5}$	12.3 $^{+12.5}_{-2.3}$	7.8 $^{+1.7}_{-3.3}$	0.14 $^{+0.31}_{-0.15}$	0.78 $^{+0.37}_{-0.33}$	0.16 $^{+0.07}_{-0.06}$	19.3 $^{+9.3}_{-1.5}$	0.72 $^{+0.07}_{-0.06}$	1800	9.5 $^{+0.3}_{-0.5}$

GWTC-2: Test of General Relativity by LIGO-Virgo

1. Residuals test



Subtract the best fit template for the event from the strain data and compute the 90% upper limit on residual SNR.

Check whether the residual SNR is consistent with SNR from noise: measure SNR from noise-only times around the event times, yielding a p -value

$$p = P(\text{SNR}_{\text{noise}}^{90\%} \geq \text{SNR}_{\text{residual}}^{90\%} \mid \text{noise})$$

TABLE III. Results of the residuals analysis (Sec. IV A). For each event, we present the SNR of the subtracted GR waveform (SNR_{GR}), the 90%-credible upper limit on the residual network SNR (SNR_{90}), a corresponding lower limit on the fitting factor (FF_{90}), and the p -value.

Events	SNR_{GR}	Residual SNR_{90}	FF_{90}	p -value
GW190408_181802	16.06	8.48	0.88	0.15
GW190412	18.23	6.67	0.94	0.30
GW190421_213856	10.47	7.52	0.81	0.07
GW190503_185404	13.21	5.78	0.92	0.83
GW190512_180714	12.81	5.92	0.91	0.44
GW190513_205428	12.85	6.44	0.89	0.70
GW190517_055101	11.52	6.40	0.87	0.69
GW190519_153544	15.34	6.38	0.92	0.65
GW190521	14.23	6.34	0.91	0.28
GW190521_074359	25.71	6.15	0.97	0.35
GW190602_175927	13.22	5.46	0.92	0.86
GW190630_185205	16.13	5.13	0.95	0.52
GW190706_222641	13.39	7.80	0.86	0.18
GW190707_093326	13.55	5.89	0.92	0.25
GW190708_232457	13.97	6.00	0.92	0.19
GW190720_000836	10.56	7.30	0.82	0.18
GW190727_060333	11.62	4.88	0.92	0.97
GW190728_064510	13.47	5.98	0.91	0.53
GW190814	25.06	6.43	0.97	0.84
GW190828_063405	16.13	8.47	0.89	0.12
GW190828_065509	9.67	6.30	0.84	0.41
GW190910_112807	14.32	5.60	0.93	0.65
GW190915_235702	13.82	8.30	0.86	0.09
GW190924_021846	12.21	5.91	0.90	0.57

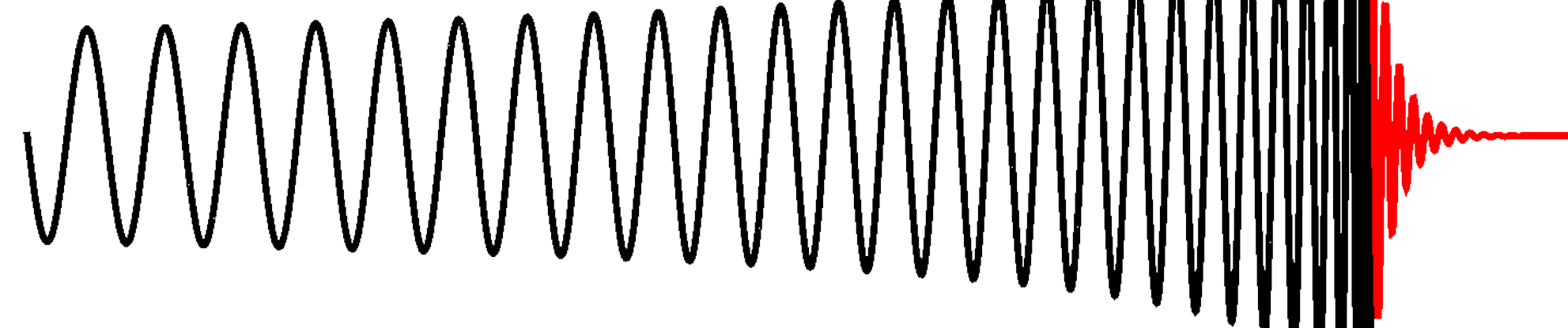
All p -values consistent with residual SNR produced by noise

No statistically significant deviations from GR

GWTC-2: Test of General Relativity by LIGO-Virgo

1. Residuals test

2. Inspiral-merger-ringdown consistency test

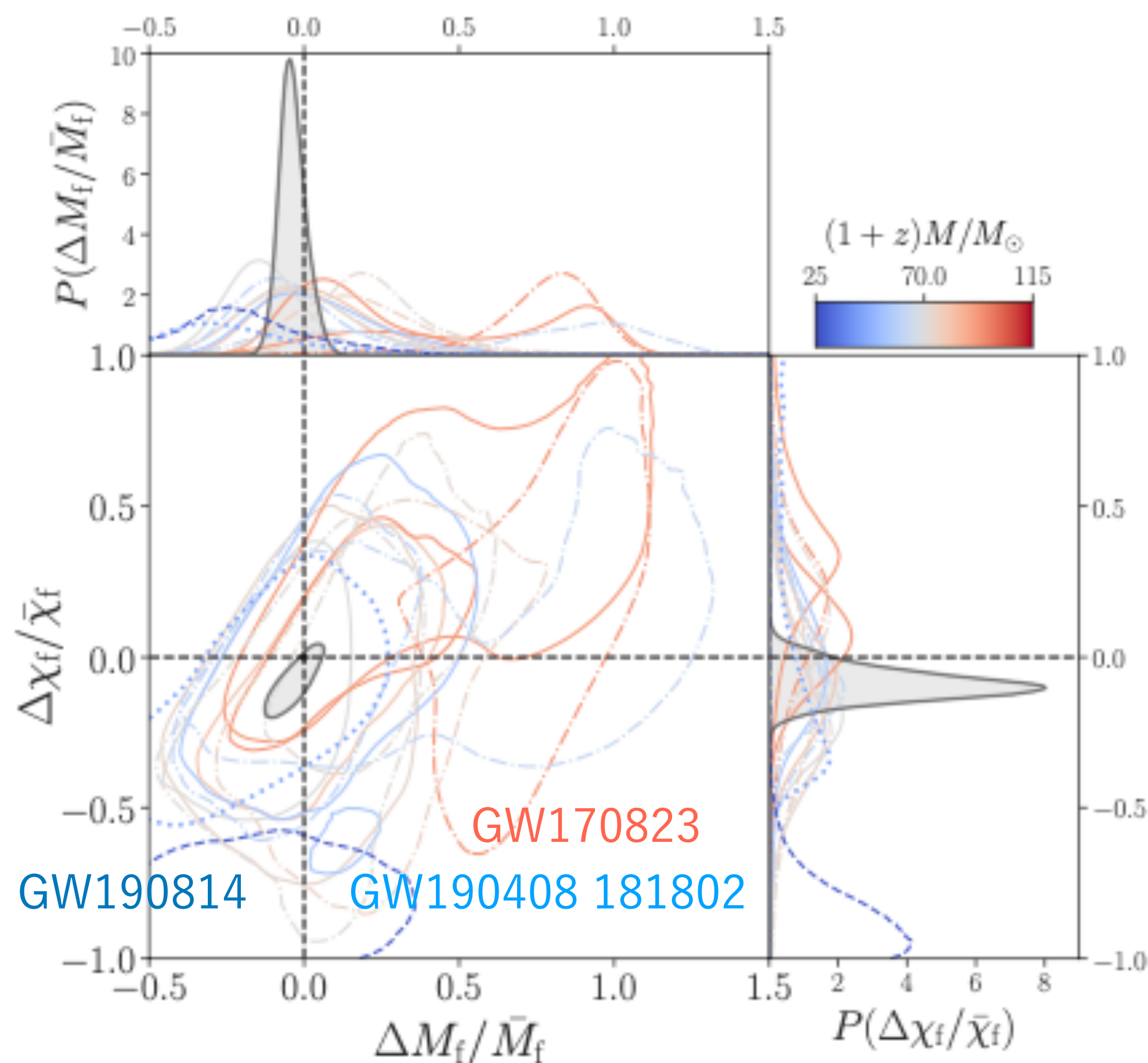


Parameter Estimation with $f < f_c$,

with $f > f_c$,

$$M_f^{\text{insp}}, \chi_f^{\text{insp}}$$

$$M_f^{\text{postinsp}}, \chi_f^{\text{postinsp}}$$



Waveform models

IMRPhenom - phenomenological PN-based models, calibrated to NR

SEOBNR - aligned-spin effective-one-body models, calibrated to NR

(note: only includes quadrupole)

◀ IMRPhenom waveform test mostly consistent, but ...

GW170823 ◀ 39.5M+29.5M, SNR@ inspiral < 8

GW190408 181802 ◀ 24.5M+18.3M, with multimodal posterior

GW190814 ◀ 23M+2.6M, large mass ratio ever

No statistically significant deviations from GR

GWTC-2: Test of General Relativity by LIGO-Virgo

1. Residuals test
2. IMR consistency test
3. Hierarchical analysis
4. Parametrized test

$$\tilde{h}(f) = A(f) e^{i\varphi(f)}$$

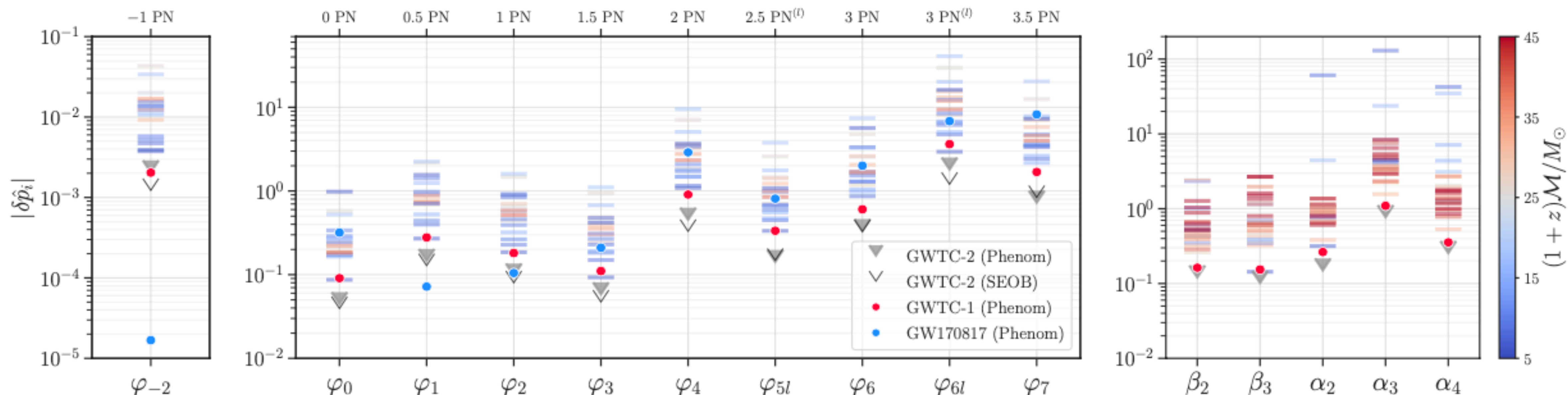
$$\begin{aligned} \varphi_{\text{inspiral}}(f) = & \varphi_{\text{ref}} + 2\pi f t_{\text{ref}} + \varphi_{\text{Newton}}(Mf)^{-5/3} + \varphi_{0.5\text{PN}}(Mf)^{-4/3} \\ & + \varphi_{1\text{PN}}(Mf)^{-1} + \varphi_{1.5\text{PN}}(Mf)^{-2/3} + \dots \end{aligned}$$

$$\{\delta\varphi_{-2}, \delta\varphi_0, \delta\varphi_1, \dots, \delta\varphi_7\} \propto f^{(i-5)/3}$$

$$\varphi_{\text{intermediate}}(f) = \eta^{-1} \left(\beta_0 + \beta_1 f + \beta_2 \log f - \frac{\beta_3}{3} f^{-3} \right)$$

$$\varphi_{\text{MR}}(f) = \eta^{-1} \left\{ \alpha_0 + \alpha_1 f - \alpha_2 f^{-1} + \frac{4}{3} \alpha_3 f^{3/4} + \alpha_4 \tan^{-1} \left(\frac{f - \alpha_5 f_{\text{RD}}}{f_{\text{damp}}} \right) \right\}$$

$$\eta = m_1 m_2 / M^2$$



No statistically significant deviations from GR

GWTC-2: Test of General Relativity by LIGO-Virgo

1. Residuals test
2. IMR consistency test
3. Hierarchical analysis
4. Parametrized test
5. Spin-induced quadrupol
6. Ringdown
7. Echoes
8. Dispersion
9. Polarizations

$$h_+(t) - ih_\times(t) = \sum_{\ell=2}^{+\infty} \sum_{m=-\ell}^{\ell} \sum_{n=0}^{+\infty} \mathcal{A}_{\ell mn} \exp\left[-\frac{t-t_0}{(1+z)\tau_{\ell mn}}\right] \exp\left[\frac{2\pi i f_{\ell mn}(t-t_0)}{1+z}\right] {}_{-2}S_{\ell mn}(\theta, \phi, \chi_f)$$

Event	Redshifted final mass (1+z)M _f [M _⊙]				Final spin χ _f				Higher modes	Overtones	
	IMR	Kerr ₂₂₀	Kerr ₂₂₁	Kerr _{HM}	IMR	Kerr ₂₂₀	Kerr ₂₂₁	Kerr _{HM}	log ₁₀ B ₂₂₀ ^{HM}	log ₁₀ B ₂₂₀ ²²¹	log ₁₀ O _{GR} ^{modGR}
GW150914	68.8 ^{+3.6} _{-3.1}	62.7 ^{+19.0} _{-12.1}	71.7 ^{+13.2} _{-12.5}	80.3 ^{+20.1} _{-21.7}	0.69 ^{+0.05} _{-0.04}	0.52 ^{+0.33} _{-0.44}	0.69 ^{+0.18} _{-0.36}	0.83 ^{+0.13} _{-0.45}	0.03	0.63	-0.34
GW170104	58.5 ^{+4.6} _{-4.1}	56.2 ^{+19.1} _{-11.6}	61.3 ^{+16.7} _{-13.2}	104.3 ^{+207.7} _{-43.1}	0.66 ^{+0.08} _{-0.11}	0.26 ^{+0.42} _{-0.24}	0.51 ^{+0.34} _{-0.44}	0.59 ^{+0.34} _{-0.51}	0.26	-0.20	-0.23
GW170814	59.7 ^{+3.0} _{-2.3}	46.1 ^{+133.0} _{-33.6}	56.6 ^{+20.9} _{-11.1}	171.2 ^{+268.7} _{-143.5}	0.72 ^{+0.07} _{-0.05}	0.52 ^{+0.42} _{-0.47}	0.47 ^{+0.40} _{-0.42}	0.54 ^{+0.41} _{-0.48}	0.04	-0.19	-0.11
GW170823	88.8 ^{+11.2} _{-10.2}	73.8 ^{+26.8} _{-23.7}	79.0 ^{+21.3} _{-13.2}	103.0 ^{+133.1} _{-46.7}	0.72 ^{+0.09} _{-0.12}	0.46 ^{+0.40} _{-0.41}	0.36 ^{+0.38} _{-0.32}	0.74 ^{+0.22} _{-0.61}	0.02	-0.98	-0.07
GW190408_181802	53.1 ^{+3.2} _{-3.4}	22.4 ^{+253.0} _{-11.1}	46.6 ^{+18.8} _{-10.9}	127.4 ^{+327.7} _{-107.6}	0.67 ^{+0.06} _{-0.07}	0.45 ^{+0.45} _{-0.40}	0.36 ^{+0.46} _{-0.33}	0.46 ^{+0.47} _{-0.41}	-0.05	-1.02	-0.02
GW190512_180714	43.4 ^{+4.1} _{-2.8}	37.6 ^{+48.9} _{-22.4}	36.7 ^{+19.3} _{-24.8}	99.4 ^{+247.6} _{-66.5}	0.65 ^{+0.07} _{-0.07}	0.41 ^{+0.47} _{-0.37}	0.45 ^{+0.40} _{-0.39}	0.77 ^{+0.20} _{-0.66}	0.09	-0.42	0.03
GW190513_205428	70.8 ^{+12.2} _{-6.9}	55.5 ^{+31.5} _{-42.1}	68.5 ^{+28.2} _{-11.8}	88.7 ^{+250.0} _{-41.9}	0.69 ^{+0.14} _{-0.12}	0.38 ^{+0.48} _{-0.34}	0.31 ^{+0.53} _{-0.28}	0.59 ^{+0.34} _{-0.52}	0.09	-0.54	-0.05
GW190519_153544	148.2 ^{+14.5} _{-15.5}	120.7 ^{+39.7} _{-21.5}	125.9 ^{+24.3} _{-21.7}	155.4 ^{+84.4} _{-42.5}	0.80 ^{+0.07} _{-0.12}	0.42 ^{+0.41} _{-0.36}	0.52 ^{+0.25} _{-0.40}	0.70 ^{+0.21} _{-0.50}	0.21	-0.00	-0.11
GW190521	259.2 ^{+36.6} _{-29.0}	282.2 ^{+50.0} _{-61.9}	284.0 ^{+40.4} _{-43.9}	299.3 ^{+57.7} _{-62.4}	0.73 ^{+0.11} _{-0.14}	0.76 ^{+0.14} _{-0.38}	0.78 ^{+0.10} _{-0.22}	0.80 ^{+0.13} _{-0.30}	0.12	-0.86	-0.50
GW190521_074359	88.1 ^{+4.3} _{-4.9}	83.0 ^{+24.0} _{-17.2}	86.4 ^{+14.1} _{-14.8}	105.9 ^{+20.8} _{-26.4}	0.72 ^{+0.05} _{-0.07}	0.57 ^{+0.31} _{-0.49}	0.67 ^{+0.17} _{-0.34}	0.87 ^{+0.09} _{-0.39}	-0.04	1.29	-0.27
GW190602_175927	165.6 ^{+20.5} _{-19.2}	156.4 ^{+71.4} _{-30.6}	160.0 ^{+37.4} _{-31.2}	261.7 ^{+84.4} _{-91.5}	0.71 ^{+0.10} _{-0.13}	0.34 ^{+0.41} _{-0.31}	0.46 ^{+0.31} _{-0.39}	0.79 ^{+0.14} _{-0.49}	0.61	-1.56	0.32
GW190706_222641	173.6 ^{+18.8} _{-22.9}	136.0 ^{+52.0} _{-29.3}	152.5 ^{+37.8} _{-28.4}	184.0 ^{+139.2} _{-55.8}	0.80 ^{+0.08} _{-0.17}	0.41 ^{+0.42} _{-0.37}	0.55 ^{+0.31} _{-0.45}	0.68 ^{+0.26} _{-0.54}	-0.06	-0.64	-0.45
GW190708_232457	34.4 ^{+2.7} _{-0.7}	28.9 ^{+285.4} _{-17.9}	32.3 ^{+15.0} _{-12.2}	171.9 ^{+307.6} _{-147.8}	0.69 ^{+0.04} _{-0.04}	0.47 ^{+0.45} _{-0.42}	0.34 ^{+0.44} _{-0.31}	0.43 ^{+0.51} _{-0.39}	-0.11	-0.17	-0.02
GW190727_060333	100.0 ^{+10.5} _{-10.0}	78.7 ^{+45.7} _{-66.4}	88.8 ^{+25.7} _{-16.0}	107.4 ^{+112.1} _{-42.7}	0.73 ^{+0.10} _{-0.10}	0.53 ^{+0.42} _{-0.47}	0.45 ^{+0.39} _{-0.41}	0.71 ^{+0.24} _{-0.59}	-0.02	-1.65	-0.40
GW190828_063405	75.9 ^{+6.0} _{-5.2}	71.2 ^{+35.8} _{-55.5}	69.6 ^{+22.0} _{-17.3}	99.0 ^{+166.0} _{-49.1}	0.76 ^{+0.06} _{-0.07}	0.72 ^{+0.25} _{-0.62}	0.65 ^{+0.27} _{-0.55}	0.92 ^{+0.06} _{-0.74}	0.05	-0.72	-0.05
GW190910_112807	97.3 ^{+9.4} _{-7.1}	112.2 ^{+32.0} _{-31.7}	107.7 ^{+28.6} _{-27.4}	137.1 ^{+59.5} _{-31.4}	0.70 ^{+0.08} _{-0.07}	0.76 ^{+0.18} _{-0.55}	0.75 ^{+0.17} _{-0.46}	0.91 ^{+0.07} _{-0.27}	-0.10	-0.64	-0.40
GW190915_235702	75.0 ^{+7.7} _{-7.3}	38.3 ^{+335.1} _{-27.4}	63.0 ^{+19.1} _{-9.9}	137.3 ^{+324.1} _{-96.2}	0.71 ^{+0.09} _{-0.11}	0.52 ^{+0.43} _{-0.46}	0.27 ^{+0.40} _{-0.24}	0.55 ^{+0.39} _{-0.49}	0.06	-0.37	-0.04

No significant evidence for higher-mode in ringdown part

Ringdown GW search using Auto-Regressive model

AR model

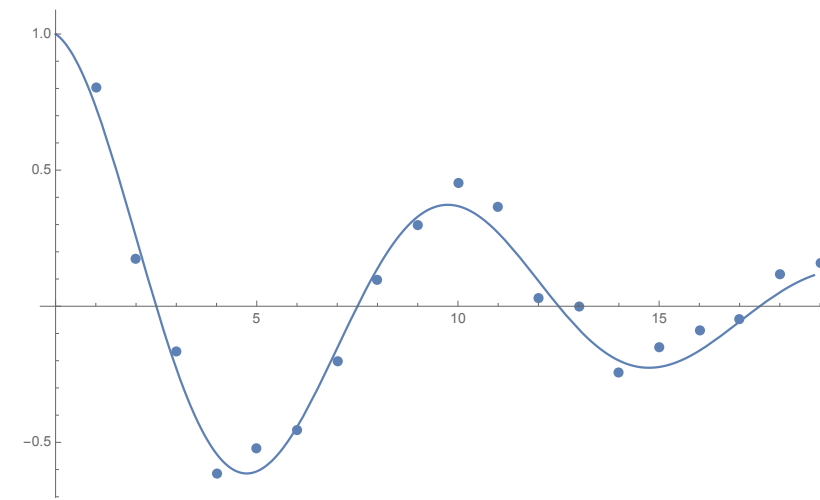
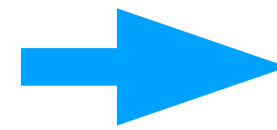
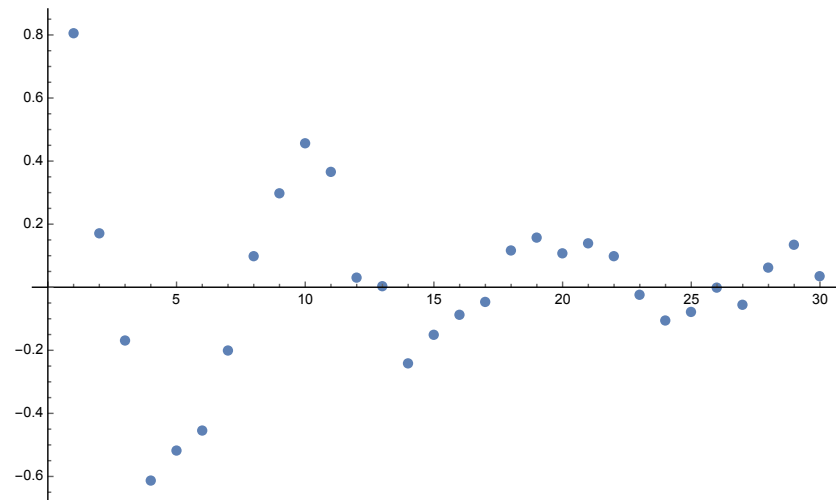
$$\begin{aligned}
 x_n &= a_1 x_{n-1} + a_2 x_{n-2} + \cdots + a_M x_{n-M} + \varepsilon_n \\
 &= \sum_{j=1}^M a_j x_{n-j} + \varepsilon
 \end{aligned}$$

e.g. $x_n = Ae^{-rn\Delta t} \cos(\omega n\Delta t)$

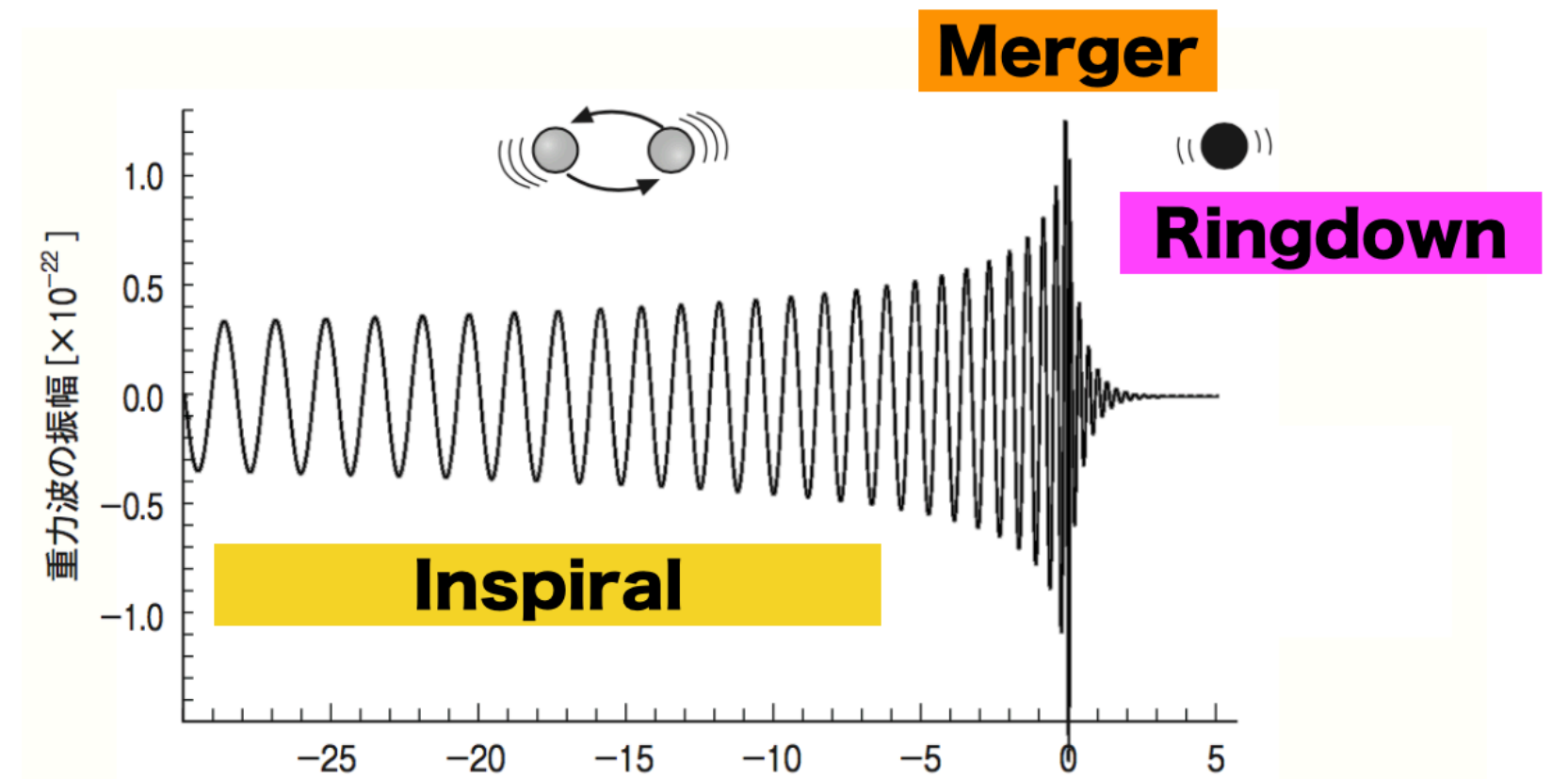
$$Z_1 = e^{-(r-j\omega)\Delta t}$$

$$Z_2 = e^{-(r+j\omega)\Delta t}$$

$$\rightarrow x_n = \frac{A}{2}(Z_1^n + Z_2^n) = (Z_1 + Z_2)x_{n-1} - Z_1 Z_2 x_{n-2}$$



can be applied also to noisy data by adjusting M



Ringdown GW search using Auto-Regressive model

AR model

$$x_n = a_1 x_{n-1} + a_2 x_{n-2} + \cdots + a_M x_{n-M} + \varepsilon_n$$

$$= \sum_{j=1}^M a_j x_{n-j} + \varepsilon$$

- find a_j (Burg method)
- find M (FPE final prediction error method)
- re-construct wave signal from fitted function
- apply FFT with arbitrary precision.

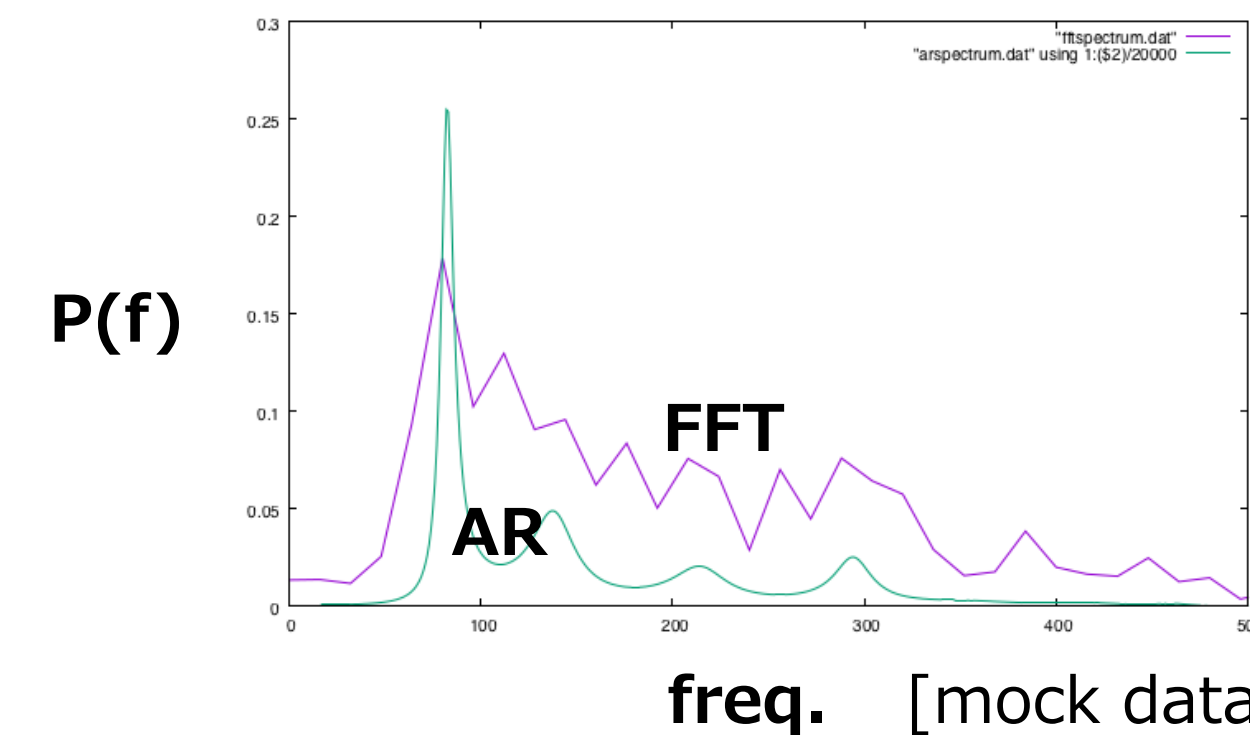
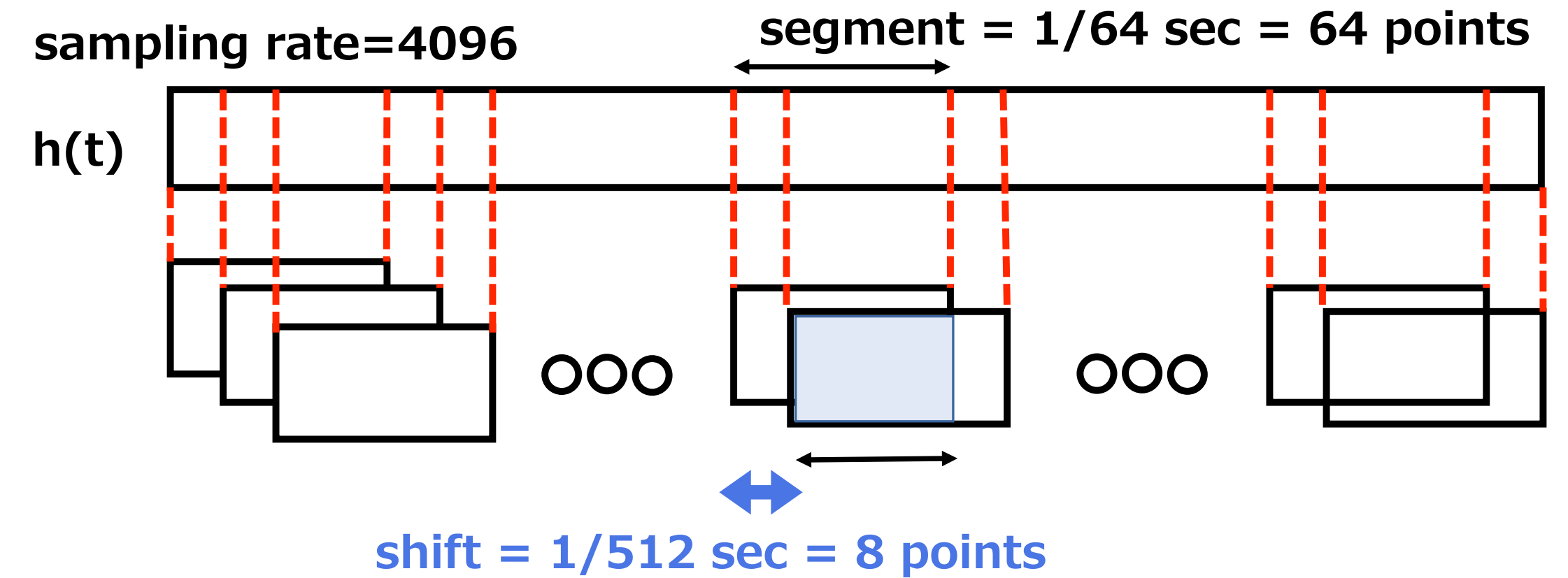
power spectrum

$$p(f) = \frac{\sigma^2}{\left| 1 - \sum_{j=1}^M a_j e^{-I2\pi j f \Delta t} \right|^2}$$

characteristic eq.

$$f(z) = 1 - \sum_{j=1}^M a_j z^j = 0$$

$|z_k|$ says amplitude,
 $\arg(z_k)$ says frequency.



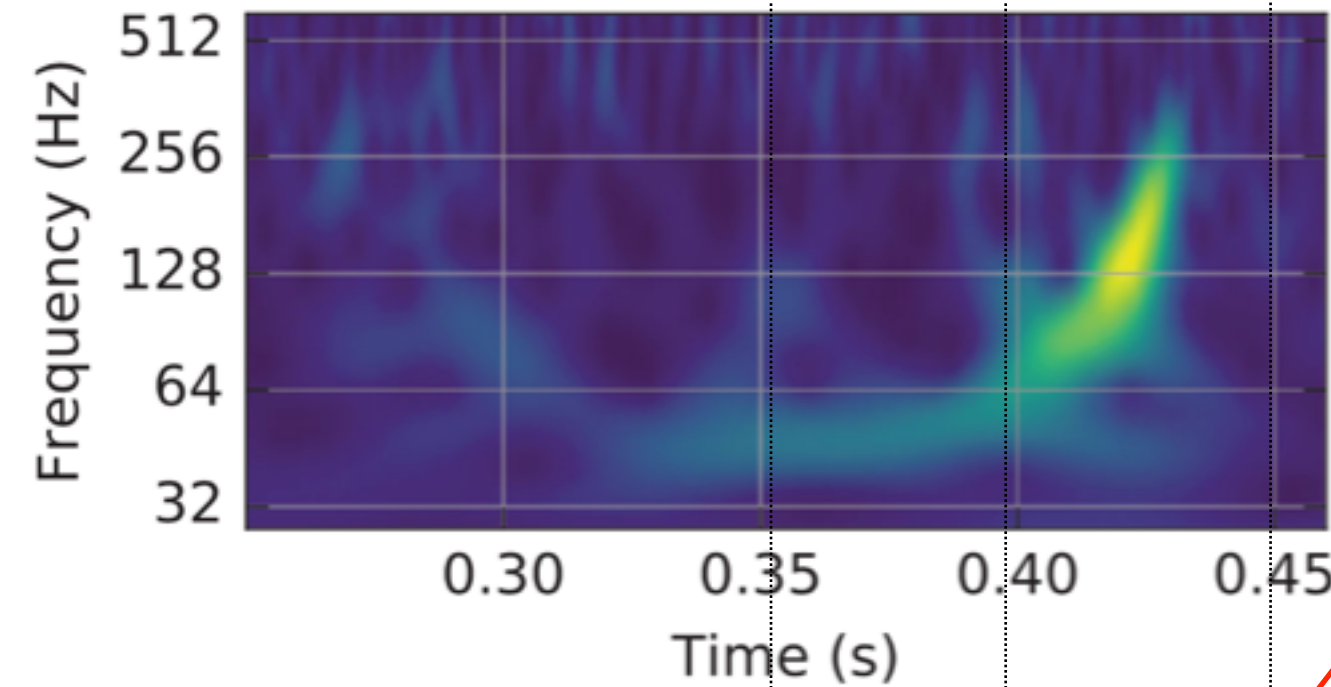
The order M can be fixed at 2~8.

**Even for short segment,
AR model shows precise
power-spectrum.**

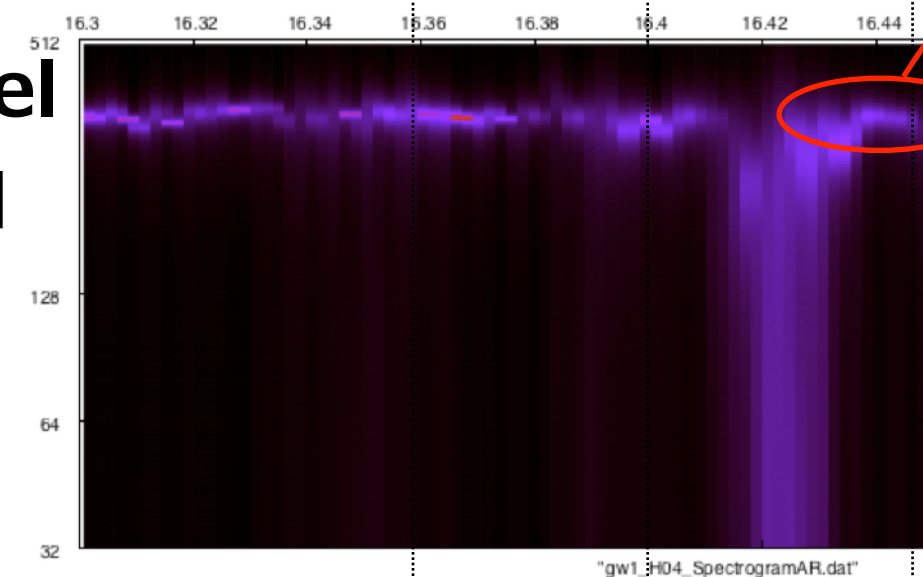
Ringdown GW search using Auto-Regressive model

GW150914 case

LIGO paper



AR model Hanford



$f_{220} = 249.4 \text{ Hz}, f_{221} = 244.0 \text{ Hz}, f_{222} = 233.7 \text{ Hz}$
 $f_{210} = 349.3 \text{ Hz}, f_{211} = 207.1 \text{ Hz}, f_{200} = 231.9 \text{ Hz}$
 $f_{330} = 395.3 \text{ Hz}, f_{331} = 392.1 \text{ Hz}, f_{332} = 386.3 \text{ Hz}$
 $f_{320} = 355.9 \text{ Hz}, f_{310} = 322.1 \text{ Hz}, f_{300} = 293.9 \text{ Hz}$

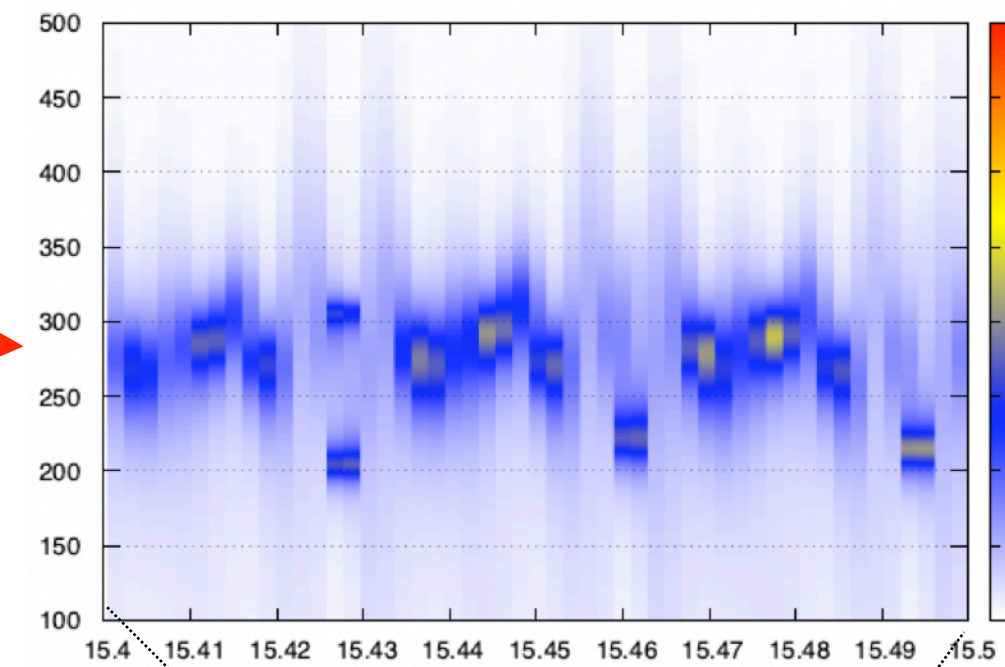
4096 sampling rate

150-450 Hz filter

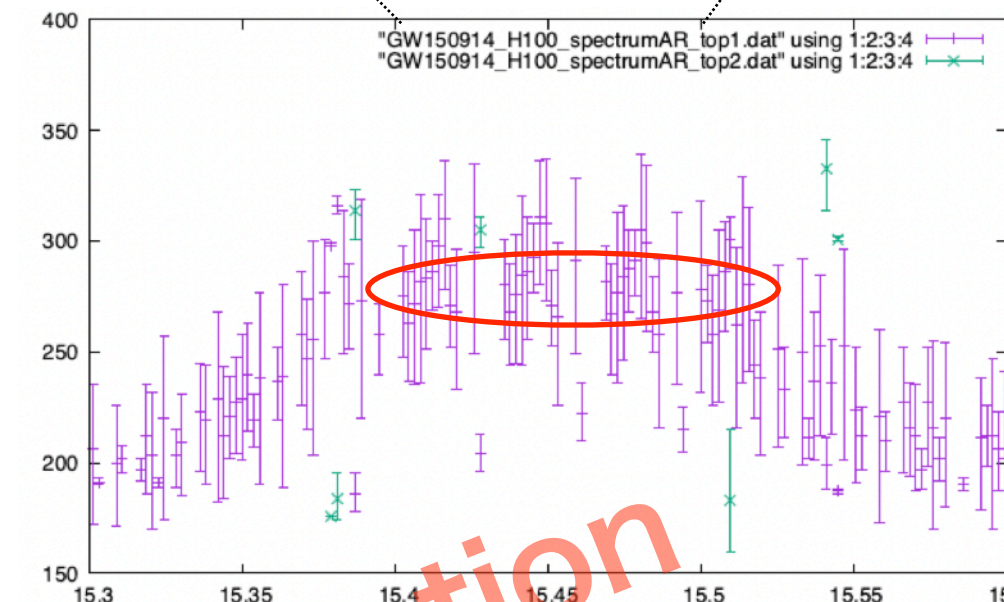
1 segment = 1/64 sec = 64 points

1 shift = 1/512 sec = 8 points

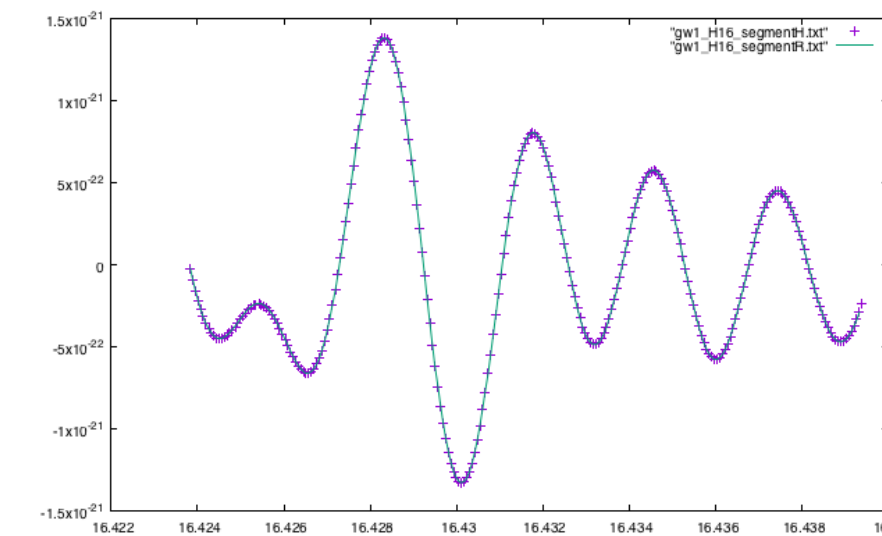
freq [Hz]



▲ merger time



In Preparation



AR-method enables us to extract waves from original signal without preparing any wave templates.

AR-method can be an alternative approach to test general relativity.

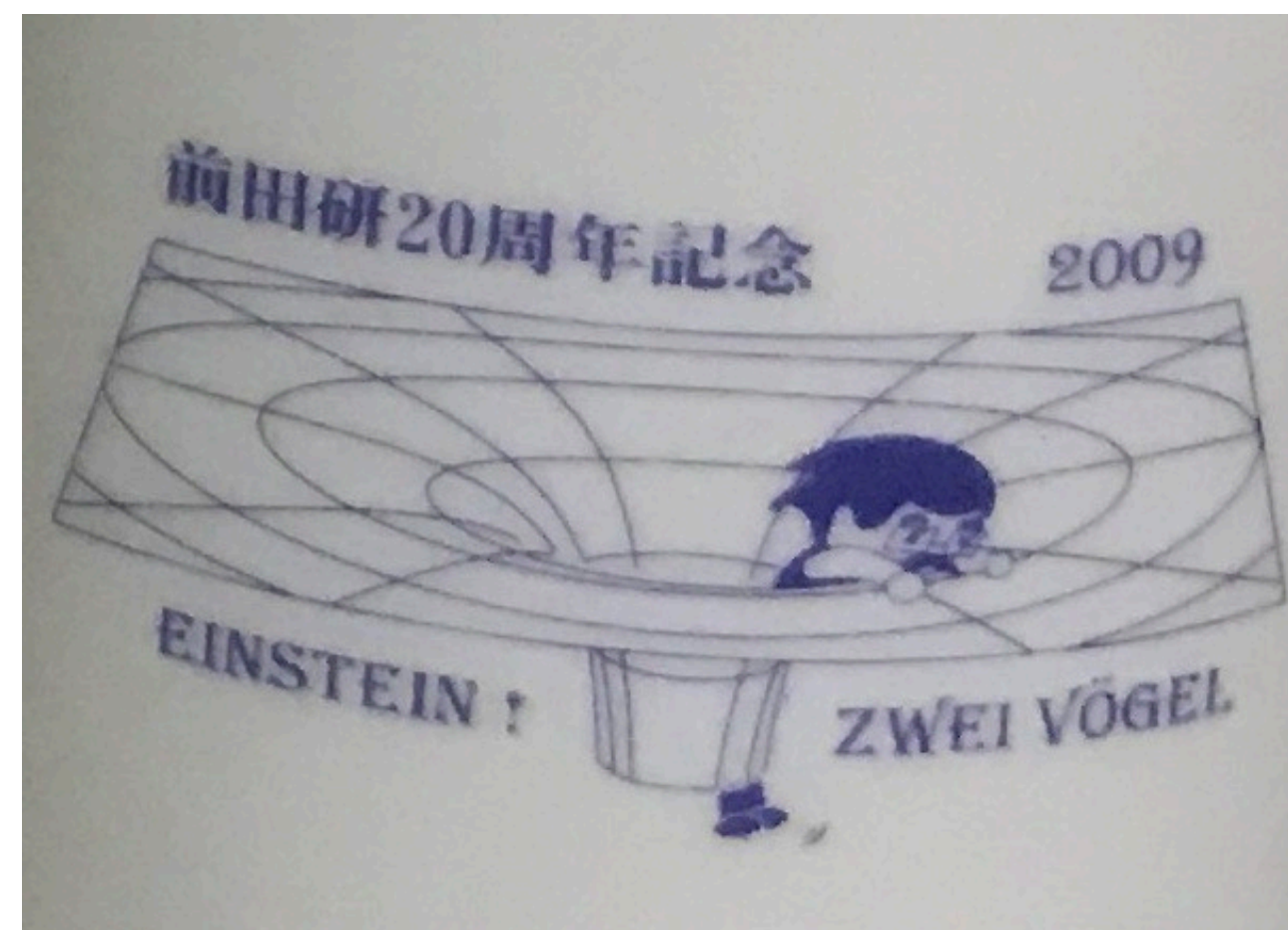
Congratulations Maeda-san, for your 70th birthday



YOU MUST BUY THEM (not from me)

You left various footprints in GR, but also you made continuous contributions for growing GR community in Japan, in the Asia, and of course in the world.

As Roger Penrose received Nobel Prize at his age 89, the theorists have to live long. The next task for you is to develop a light-speed rocket or a way to escape from the strong gravity region.



Hisaaki Shinkai (Osaka Inst. Tech.)

